

SECTION III

TITLE PAGES OF PUBLISHED PAPERS

(JULY 1977-JUNE 1978)

Observation of Hole States at High Excitation in (p,t) Reactions

G. M. Crawley, W. Benenson, D. Weber, and B. Zwieglinski^(a)

Cyclotron Laboratory and Department of Physics, Michigan State University, East Lansing, Michigan 48824

(Received 18 August 1977)

A peak about 2 MeV wide is observed at $E_x \sim 8-9$ MeV in six even-even tin isotopes and at lower excitation in ^{104}Cd and ^{102}Pd in the (p,t) reaction at 42 and 45 MeV. The excitation energy of the peak and its width increase with increasing neutron number. The peak may arise from two-neutron pickup from the lower-lying gpf shell. Distorted-wave Born-approximation calculations agree well with the angular distributions and indicate that 45% of the total strength is observed experimentally.

The manner of spreading of simple states into an underlying background of more complex states remains one of the important questions in nuclear physics.¹ One method of studying this problem is by pickup reactions particularly at high excitation energies, at which the level density is substantial.^{2,3} Neutron hole states with spin-parity $\frac{9}{2}^+$, $\frac{1}{2}^-$, and $\frac{3}{2}^-$ and with significant spectroscopic factors have been observed at about 5 MeV of excitation in the odd- A tin isotopes in single-neutron pickup reactions.⁴⁻⁶ In the present (p,t) experiment, which was motivated by a search for high-lying pairing resonances,⁷ a peak was observed at an excitation energy of about 8 to 9 MeV in a number of tin isotopes. One plausible explanation for this peak is that it arises from two-neutron hole states in the major shell consisting of $1g_{9/2}$, $2p_{1/2}$, $2p_{3/2}$, and possibly $1f_{5/2}$ levels.⁸

Because the pairing resonances were predicted to occur at $70/A^{1/3}$ MeV, i.e., about 14.1 MeV for ^{122}Sn , using a degenerate-harmonic-oscillator model, the first measurements were carried out with a ^{122}Sn target at a proton bombarding energy of 45 MeV, and the tritons were detected in a standard counter telescope consisting of three Si detectors. This arrangement permitted the study of ^{120}Sn up to an excitation energy of about 17 MeV. No structure was observed near 14 MeV, but a substantial "bump" was observed around 8.5 MeV excitation.

In order to study this phenomenon in more detail, the reaction $^{122}\text{Sn}(p,t)$ was repeated at a proton bombarding energy of 42 MeV using a 50-cm-long resistive-wire proportional counter backed by a plastic scintillator in the focal plane of the Enge spectrograph. This arrangement gave very clear identification of the tritons but was restricted to measuring a range of triton energies from about 32.5 to 21.5 MeV. Again an enhancement of the cross section was observed near 8.5 MeV in ^{120}Sn , quite consistent with the

observations at 45 MeV using the silicon counter telescope. This excluded the possibility that the effect had an instrumental origin. A search of the literature showed that indications of similar structure is present in previously published (p,t) spectra^{9,10} but was not discussed.

The (p,t) experiment was continued at 42 MeV on the even tin isotopes, ^{124}Sn , ^{122}Sn , ^{120}Sn , ^{118}Sn , and ^{116}Sn , using the Enge spectrograph. The energy resolution was dominated by the target thicknesses which ranged from 0.5 to 5 mg/cm². The spectra obtained from these measurements at a laboratory angle of 16° are plotted in Fig. 1, using the same absolute energy scale. A peak, about 2 MeV wide at an excitation energy between 8 and 9 MeV is observed in all the Sn isotopes studied. In addition the reactions $^{106}\text{Cd}(p,t)$ and $^{104}\text{Pd}(p,t)$ were examined. Enhancement was also seen in ^{104}Cd and ^{102}Pd but at a lower excitation energy. In these two cases, fine structure was evident on top of an overall increase in cross section. In order to check for fine structure in the tin isotopes, a few runs were taken with a 280- $\mu\text{g}/\text{cm}^2$ -thick ^{124}Sn target with an energy resolution of about 50 keV full width at half-maximum. No fine structure was observed.

The excitation energies of the peaks and the full width at half-maximum of the broad structure are given in Table I. The excitation energy of the peak increases with the addition of neutrons. In addition the width of the peak increases from about 1.9 MeV in ^{114}Sn to 2.7 MeV in ^{122}Sn , and the peak becomes more asymmetric for the heavier tin isotopes.

A possible explanation of this feature is that it arises from the pickup of two neutrons from the lower-lying, filled, major shell which contains the single-particle orbits $1g_{9/2}$, $2p_{1/2}$, $2p_{3/2}$, and $1f_{5/2}$. This explanation is consistent with the observed increase in the excitation with increasing neutron number since, if coupling with other

Anomalous Optical-Model Potential for Sub-Coulomb Protons for $89 < A < 130$

C. H. Johnson

Oak Ridge National Laboratory, Oak Ridge, Tennessee 37830

and

A. Galonsky

Michigan State University, East Lansing, Michigan 48824

and

R. L. Kernell

Old Dominion University, Norfolk, Virginia 23506

(Received 3 October 1977)

The (p, n) cross sections for fourteen nuclei from $A = 89$ to $A = 130$ were measured from about 2.5 to 5.8 MeV in order to obtain total reaction cross sections. These cross sections disagree with optical-model predictions in that the predicted $3p$ resonance is missing near $A = 105$ and the peak near $A = 90$ is replaced by a valley. The data can be described by introducing an anomalous A dependence into the depth of the absorptive potential.

We present arguments with supporting data that certain experiments should be exploited to learn more about the optical-model potential (OMP) for protons. The experiments are to measure (p, n) cross sections for protons incident below the Coulomb barrier. Data from initial experiments of this type show that the OMP for $89 < A < 130$ has an anomalous behavior which merits more study.

A strength function $\langle \gamma_{l,J}^2 \rangle / \langle D_{l,J} \rangle$ is the ratio of the reduced particle width to level spacing averaged over the closely spaced compound-nuclear states of spin J formed by l -wave particles. Our contribution deals with protons, but first we comment on the familiar neutron strength functions.¹ Neutron single-particle states give rise to giant "size" resonances that are observed in plots of the strength function versus mass number for s waves near $A = 55$ and 160 and for p waves near $A = 95$. One can describe the resonances approximately by the OMP by "tuning" the volume of the real well to fit the resonant masses and by adjusting the imaginary part and the diffuseness to give the height and width of each resonance. As for the $A = 160$ resonance, the $3p$ resonance near $A = 95$ may be split. Although a splitting was at-

tributed to vibrational motions,² the early-found strength-function data have been questioned,¹ and recent precision total-cross-section measurements suggest that the resonance is smooth and without structure.³

We would like to emphasize the complementary information on the nucleon OMP to be obtained from protons incident below the Coulomb barrier. There is a dearth of precision sub-Coulomb data, perhaps because workers recognize the barrier's problems more than its benefits. There are problems. Resonances are difficult to resolve because the energies needed for barrier penetration are much larger than the level spacings. Even so, Bilpuch *et al.*⁴ obtained strength functions by resolving resonances for $A < 65$. For higher masses for which individual levels cannot be resolved, useful data can be obtained if the average energies and cross sections are measured accurately and the Coulomb penetrabilities are divided out to reveal the nuclear effects.

The Coulomb barrier has two beneficial effects. The first, which seems not to be fully appreciated, is that the barrier, by virtue of its height relative to the spreading width from the absorptive potential, can quasibind a single-particle

Empirical Renormalization of the One-Body Gamow-Teller β -Decay Matrix Elements in the $1s-0d$ Shell

B. A. Brown and W. Chung^(a)

Cyclotron Laboratory, Michigan State University, East Lansing, Michigan 48824

and

B. H. Wildenthal

Institut de Physique Nucléaire, 91406 Orsay, France, and Cyclotron Laboratory, Michigan State University,^(b) East Lansing, Michigan 48824

(Received 6 December 1977)

β -decay data from nuclei with $17 \leq A \leq 39$ are analyzed with full sd -space shell-model wave functions to determine the effective values of the single-particle matrix elements of the Gamow-Teller operator between all combinations of sd -shell orbitals.

A fundamental problem of nuclear physics is to understand the effects which the nuclear medium has, via mesonic exchange currents, upon the properties of the individual constituent nucleons of the nucleus. It is also of basic importance to understand the effects introduced by the necessity of treating the many-nucleon system with model-space truncations. Discussions of these effects are based on comparisons of experimental results to predictions based on the assumptions of the classical nuclear shell model and the properties of the neutron and proton in free space. Because of the difficulties inherent

in treating many active particles in the framework of the shell model, study of these problems has to date been confined primarily to "single-particle" nuclei such as (to take examples from the sd shell) ^{17}O , ^{17}F , ^{38}Ca , and ^{39}K . Our attention here is focused upon possible mesonic and truncation effects in Gamow-Teller (GT) β decay in the region $17 \leq A \leq 39$. We have been able, by taking advantage of recent advances in shell-model calculations,^{1,2} to analyze data³ from *all* the sd -shell nuclei with the same model approximations which are conventionally used for the single-particle systems, and can thereby base our

SPECTROSCOPY OF ^{16}C *

H.T. FORTUNE, R. MIDDLETON, M.E. COBERN,
G.E. MOORE, S. MORDECHAI, R.V. KOLLARITS

Physics Department, University of Pennsylvania, Philadelphia, Pennsylvania 19104, USA

and

H. NANN ‡, W. CHUNG and B.H. WILDENTHAL

Michigan State University, East Lansing, Michigan 48823, USA

Received 30 June 1977

The $^{14}\text{C}(t, p)^{16}\text{C}$ reaction locates five new states in ^{16}C , at excitation energies of 3020 ± 15 , 3983 ± 10 , 4083 ± 10 , 4136 ± 10 and 6109 ± 15 keV, in addition to the g.s. and 1.76 MeV states. The 3.02 and 3.98 MeV states appear to be the second 0^+ and 2^+ 2p-2h states, respectively. The 4.14 MeV state has $J^\pi = 4^+$ and the 6.11 MeV state has $J^\pi = 2^+$, 3^- , or 4^+ .

The low-lying $T = 2$ levels in mass 16 should be dominated by the configuration $(sd)^2(1p^{1/2})^{-2}$, i.e. two-particle two-hole (2p-2h) states with $T_p = 1$, $T_h = 1$. Additional positive-parity states of 4p-4h character may also exist at relatively low excitation. Weak-coupling calculations suggest that the only 4p-4h $T = 2$ states that are important at low excitation have $T_p = 2$, $T_h = 0$, i.e. $^{20}\text{O} \otimes ^{12}\text{C}$ in weak coupling notation. The lowest negative-parity states with $T = 2$ should be 3p-3h, with $T_p = 3/2$, $T_h = 1/2$, i.e. $^{19}\text{O} \otimes ^{13}\text{C}$.

In lowest order, only the 2p-2h states can be populated via direct 2n transfer. Since the first-excited state of ^{14}C is above 6 MeV, we expect the 2p-2h states to resemble closely the spectrum one would get from an $(sd)^2$ shell-model calculation. Such a calculation produces below 6 MeV two 0^+ states, two 2^+ states, one 4^+ state, and one 3^+ state. The exact energies and wavefunctions of these levels depend on the interaction assumed but the general picture does not [1].

Because the $2s_{1/2}$ single-particle state moves down in energy relative to the $1d_{5/2}$ state as one goes to lighter nuclei, any shell-model calculation for ^{16}C will predict [1] less spacing between the first two 0^+ states than that observed in ^{18}O . Also, for a variety of interactions, the second 0^+ and the second 2^+ state are pre-

dicted [1] to have very little (t, p) strength – due to nearly exact cancellation between the two dominant components in their wavefunctions ($1d_{5/2}^2$ and $2s_{1/2}^2$ for the 0^+ and $1d_{5/2}^2$ and $1d_{5/2}2s_{1/2}$ for the 2^+).

We have investigated the $T = 2$ states in ^{16}C by making use of the $^{14}\text{C}(t, p)^{16}\text{C}$ reaction. The target was a gold-backed ^{14}C foil of about $50\mu\text{g}/\text{cm}^2$ enriched to about 90% in ^{14}C . Bombardments were made at triton energies of 15, 17, and 18 MeV. Outgoing protons were detected in a multi-angle spectrograph. Absorbers directly in front of the focal plane stopped all particles except protons. Displayed in fig. 1 is a spectrum from the $^{14}\text{C}(t, p)^{16}\text{C}$ reaction at 18 MeV. Only the ground state and the (2^+) state at 1.75 MeV were known previously [2]. We see at least five additional states – at excitation energies of 3020 ± 15 , 3983 ± 10 , 4083 ± 10 , 4136 ± 10 and 6109 ± 15 keV. Our energy for the first excited state is 1766 ± 10 keV. States from the $^{12}\text{C}(t, p)^{14}\text{C}$ reaction were used in the calibration. The measured Q -value for the $^{14}\text{C}(t, p)^{16}\text{C}$ (g.s.) reaction is -3015 ± 8 keV, to be compared with the value of -3012 ± 16 keV from the 1971 mass tables [3].

From their strengths alone, the g.s. and levels at 1.76, 4.14 and 6.11 MeV must be natural-parity states. Their angular distributions at 18 MeV are displayed in fig. 2, along with DWBA curves. The shapes of the angular distributions are well reproduced by the DWBA calculations, thus indicating a small contribution from

* Work supported by the National Science Foundation.

† Present address: Los Alamos Scientific Laboratory, Los Alamos, New Mexico 87544, USA.

EXCITATION OF GIANT RESONANCE IN ^{90}Zr BY INELASTIC ^6Li SCATTERING*

R. PARDO, R.G. MARKHAM, W. BENENSON, A.I. GALONSKY and E. KASHY

Cyclotron Laboratory and Physics Department, Michigan State University, East Lansing, MI 48824, USA

Received 28 September 1977

Inelastic ^6Li scattering by ^{90}Zr was measured at 74 MeV. A broad structure, which appears to be the giant quadrupole resonance, was observed at 13.8 MeV excitation energy. This observation is in agreement with previous work done with ions lighter than ^6Li .

Inelastic scattering has proven to be the main source of information on giant resonances other than the giant electric dipole resonance. A large part of this information has come from comparisons among the spectra and yields produced by different projectiles. It is logical, therefore, to extend this study beyond the present limit, the α -particle, into the heavy-ion region. Heavy ions are expected to have two advantages over the lighter ones for studies of the giant resonances with $L > 2$. These are: (1) larger incoming angular momentum and (2) lower background yield from evaporation and from other three-body reactions in the continuum. Opposed to these advantage is the relatively poorer kinematic matching conditions which reduce the yield at high excitation energies.

Although the giant quadrupole resonance (GQR) is well established at $E_x \approx 63 A^{-1/3}$ MeV, heavy-ion inelastic scattering should give one more piece of information. Evidence for giant resonances with $L > 2$ is very sparse, and no single experiment is convincing by itself. The evidence for E3 giant resonances has been summarized by Satchler [1]. The $L = 4$ component, which is predicted to lie near the GQR, has never been observed.

In this experiment ^6Li ions, inelastically scattered from a 1.0 mg/cm^2 ^{90}Zr target (97.8% enrichment), were analyzed in the focal plane of an Enge split-pole spectrograph using a charge-division wire counter. A plastic scintillator behind the wire counter gave total-energy and time-of-flight information, allowing unique identification of ^6Li ions. Events which fulfilled two-dimensional gating requirements of ΔE , E , and time-

* Work supported in part by the US National Science Foundation.

of-flight versus position were accumulated in one-dimensional position spectra. Beams of 5–20 enA of 74 MeV $^6\text{Li}^{3+}$ ions were provided by the MSU cyclotron. The overall resolution was approximately 175 keV FWHM for the low-lying states of ^{90}Zr . The major contribution to the resolution came from the target thickness. An angular distribution was taken in 2° steps from 11° to 25° . Angles forward of 11° were not useful because of scattering from hydrogen in the target and because of the large tail from elastic scattering.

Fig. 1 shows the spectrum of events accumulated at

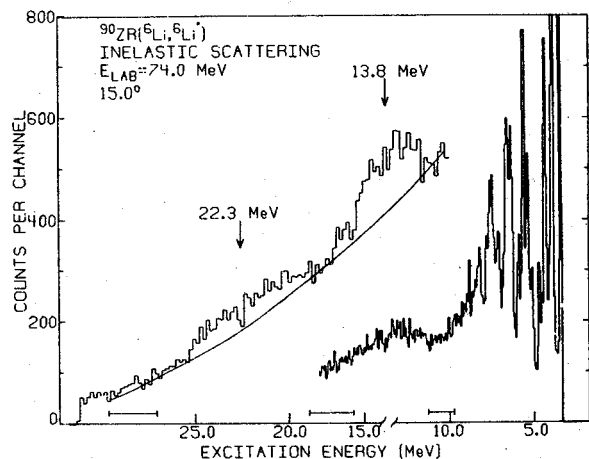


Fig. 1. Spectra of events observed in $^{90}\text{Zr}(^6\text{Li}, ^6\text{Li})$. The spectrum spanning the energy region of $E_x > \approx 10$ MeV has an average slope of 0.19 MeV/ch. The spectrum spanning the lower excitation energy region has an average slope of 0.03 MeV/ch. The connected arrows span the energy region where the ^7Li breakup mechanism (see text) is expected to contribute events.

ON THE VALIDITY OF A MODEL FOR DEEP INELASTIC REACTIONS[☆]

Shang-fang TSAI

School of Physics and Astronomy, University of Minnesota, Minneapolis, Minnesota 55455, USA

and

G.F. BERTSCH

Cyclotron Laboratory and Physics Department, Michigan State University, East Lansing, Michigan 48824, USA

Received 29 September 1977

Revised manuscript received 28 December 1977

The inclusive inelastic proton cross section on ^{208}Pb in the energy-loss range of 10–20 MeV cannot be reasonably accounted for by one-step reactions, contrary to a claim of a recent article. We make a sum rule analysis to expose the problem as clearly as possible.

The question of whether inelastic scattering with large energy losses comes mainly from single or multiple collisions is important to our understanding of nuclear reactions. A test case is the reaction $^{209}\text{Bi}(p, p')$ at $E_p = 62$ MeV [1], which has been analyzed by several authors within the distorted-wave Born approximation theory of direct reactions [2–5]. Conclusions were radically different. Tamura et al. [5] found that virtually all of the cross section with energy loss 10 to 20 MeV is due to direct one-step reactions. Bertsch and Tsai [3,4] found that only about 25% of the experimental strength could be accounted for by one-step reactions. In a preliminary version of this letter we tried to understand the discrepancy by focussing on the different descriptions of the target excitations, and their compatibility with sum rules. Drs. Tamura and Udagawa have since informed us [11] that the form factor they actually used was twice the quoted value. We will show that their quoted form factor is quite reasonable, and thus our own original conclusion stands.

In Tamura et al. the excitations are taken to be non-interacting particle–hole states, and the transition

potential is of the form given by the collective model. This treatment can be considered as a simple approximation to the more complete and detailed random phase approximation (RPA) response-function theory. The RPA theory based on the Skyrme Hartree–Fock hamiltonian was used by Bertsch and Tsai to describe the target excitations. In ref. [3] we fit the transition densities to the collective model, as is done by Tamura et al. In ref. [4] the collective form factor was replaced by the actual transition density, but there was little effect on the final results.

We wish to emphasize the possible explanation given by Tamura et al. for the discrepancy between the two calculations, that an insufficient number of particle–hole states was considered in ref. [3], is incorrect. By including all particle–hole configurations up to 40 MeV in excitation, we have exhausted all the particle–hole states used by Tamura et al. and therefore cannot miss any strength available in the non-interacting particle–hole model. In fact, due to the known attractive nature of the isoscalar particle–hole interaction, more strength is found to lie in the region of 10 to 20 MeV using RPA than using the non-interacting particle–hole model.

To narrow down possible difference in the models, we will examine the $\beta_L(E)$ predicted by the two mod-

[☆] Work supported under USERDA Contract E(11-1)-1764 and National Science Foundation.

A MICROSCOPIC CALCULATION OF ANGULAR AND ENERGY DISTRIBUTIONS OF LIGHT FRAGMENTS IN DEEPLY INELASTIC HEAVY-ION REACTIONS

D. AGASSI¹ and H.A. WEIDENMÜLLER²

Max-Planck-Institut für Kernphysik, Heidelberg, W. Germany

and

C.M. KO

Department of Physics, Michigan State University, East Lansing, Michigan, USA

Received 9 November 1977

A random-matrix model for the form factors connecting channels corresponding to high intrinsic excitation energy of either fragment is used to calculate energy-averaged cross sections in deeply inelastic heavy-ion reactions. The distribution of the form factors is determined microscopically. The calculation yields differential cross sections without any fit parameters. Results for Kr- and Bi-induced reactions are compared with the data.

1. Purpose. In this letter, we present the first results of a microscopic calculation of the distribution in angle and energy of reaction products observed in deeply inelastic heavy-ion collisions (DIC). These calculations were stimulated by the success of phenomenological friction models [1] in accounting for some aspects of the data. It was our aim to replace the phenomenological friction coefficients of these models, as well as the diffusion constants used in some more recent versions [2] by expressions derived from a microscopic input.

Some authors [3] have developed a microscopic theory of DIC based on the use of linear response theory, on the description of intrinsic excitation in terms of a temperature, and on the Einstein relation connecting friction and diffusion constants. No microscopic calculation of transport coefficients has yet been performed in this frame, however.

Moreover, it is not obvious a priori that the input

just mentioned does apply to DIC. Therefore, we have not made use of this set of assumptions, but have taken instead a statistical input based on a random-matrix model. This is similar in spirit to the approach taken in refs. [4], although our theoretical method is quite different from and, we believe, more stringent than that of refs. [4].

2. Input. We decompose the hamiltonian H in the form

$$H = H_{\text{rel}}(R) + H_0(\xi) + V_{\text{int}}(R, \xi). \quad (1)$$

Here, $H_{\text{rel}}(R)$ is the hamiltonian of relative motion of the two fragments in a heavy-ion collision. The distance between the two cm's is denoted by R . The operator $H_{\text{rel}}(R)$ consists of a kinetic-energy term which contains the reduced mass, and of a potential-energy term containing the sum of the Coulomb potential, and of the nuclear potential which was taken to be the proximity potential in the form parametrised in ref. [5].

The operator $H_0(\xi)$ is the sum of the intrinsic hamiltonians of the separated fragments, with eigenvalues ϵ_s and eigenstates $|s\rangle$. The states $|s\rangle$ are products of eigenstates of the two fragments, coupled to total spin I .

¹ On leave from Weizmann Institute of Science, Rehovot, Israel. Supported by Minerva, Present address: Department of Physics, University of Rochester, Rochester, NY., USA.

² Present address: Department of Theoretical Physics, Oxford University, Oxford, UK.

OBSERVATION OF THE $T = 4$ AND $T = 5$ COMPONENTS OF THE GIANT GAMOW-TELLER RESONANCE IN THE (${}^3\text{He}$, t) REACTION AT 130 MeV

Aaron GALONSKY

*Michigan State University, East Lansing, MI 48824, USA
and KFA, 5170 Jülich, Germany*

and

J.P. DIDELEZ, A. DJALOEIS and W. OELERT
KFA, 5170 Jülich, Germany

Received 15 February 1978

Broad peaks around 9 and 19 MeV excitation energy have been observed in the ${}^{90}\text{Zr}({}^3\text{He}, \text{t}){}^{90}\text{Nb}$ reaction at 130 MeV. These peaks are interpreted as the $T = 4$ and $T = 5$ components, respectively, of a giant Gamow-Teller transition.

Since the pioneering (p, n) experiments of Anderson and Wong [1], giant resonances have been seen in charge-exchange, or $\Delta T = 1$, reactions. These giant isovector resonances arise in transitions to the isobaric analog states (IAS) of target ground states. Except for T_Z , the nuclear quantum numbers do not change in an IAS transition. In the language of β -decay we have a superallowed or giant Fermi transition.

Following the discovery of IAS a giant Gamow-Teller, or spin-flip, transition in charge-exchange reactions was predicted [2]. Evidence was reported [3] for such a resonance in neutron spectra from the ${}^{90}\text{Zr}(p, n){}^{90}\text{Nb}$ reaction at 45 MeV. We have observed very similar structure in triton spectra produced in the ${}^{90}\text{Zr}({}^3\text{He}, \text{t}){}^{90}\text{Nb}$ reaction at 130 MeV. Furthermore, the triton spectra have an additional resonance which we interpret as a higher isospin component of the giant Gamow-Teller resonance.

The data were taken with a pair of $\Delta E-E$ telescopes, each composed of a commercial 2 mm silicon detector and a thick, home-made [4] germanium detector. With Ortec particle-identifier modules tritons were well separated from other particle types. The angular range 10° to 35° was observed at 1° intervals. For the smaller angles the high-resolution ${}^3\text{He}$ beam from the Jülich cyclotron was used; for the larger an-

gles, where the yields were lower, the achromatic, higher-intensity beam was used. For these two beams typical currents were 10 nA and 80 nA, respectively.

Fig. 1 shows a triton spectrum obtained with each of the two telescopes. The reaction angles are 15° and 30° . At 15° the ${}^3\text{He}$ beam had the higher resolution and at 30° the lower resolution. The two spectra have the same features. The most prominent of these features is the IAS, or giant Fermi resonance, at 5.1 MeV excitation energy in ${}^{90}\text{Nb}$. It is the lowest $T = 5$ state, a 0^+ state, in a $T_Z = 4$ nucleus. By mixing with $T = 4$ states via the relatively weak Coulomb force, it remains narrow. A few MeV higher, centered around 8.5 MeV, is the broad, $T = 4$, 1^+ giant Gamow-Teller resonance found in the (p, n) experiment [3]. About 10 MeV above this state, at ≈ 18.5 MeV, is another broad bump, a bump not previously reported. We suggest that it is the $T = 5$ component of the giant Gamow-Teller transition which is being seen here.

Two obvious questions can be raised about this interpretation. Why is this $T = 5$ state broad in contrast to the $T = 5$ IAS, and is the magnitude of the observed isospin splitting, ≈ 10 MeV, correct? At 13.5 MeV higher excitation energy, many 1^+ , $T = 5$ states must be available for mixing via the strong force. The result, as for the $T = 4$ component, is a broad bump. As for

THE MASS OF ^{15}B VIA A THREE-PROTON STRIPPING REACTION

T.S. BHATIA¹, H. HAFNER², J.A. NOLEN Jr.³, W. SAATHOFF,
R. SCHUHMACHER, R.E. TRIBBLE⁴, G.J. WAGNER and C.A. WIEDNER
Max-Planck-Institut für Kernphysik, Heidelberg, Federal Republic of Germany

Received 17 April 1978

The isotope ^{15}B was produced via the reaction $^{48}\text{Ca}(^{18}\text{O}, ^{15}\text{B})^{51}\text{V}$. The Q -value and mass excess were determined to be -21.76 ± 0.05 MeV and 28.96 ± 0.05 MeV, respectively. A search for the isotope ^{14}Be was unsuccessful.

Mass measurements of the $T_z = 5/2$ nuclei ^{21}O [1, 2], ^{19}N [3], and ^{17}C [4] have recently been reported, leaving ^{15}B as the only particle-stable $T_z = 5/2$ neutron-rich nucleus with unknown mass. In this letter we report the results of a mass measurement of ^{15}B via the $^{48}\text{Ca}(^{18}\text{O}, ^{15}\text{B})^{51}\text{V}$ reaction. Two other attempts to determine the mass of ^{15}B were both inconclusive [5, 6]. Previous mass measurements of sd-shell $T_z = 5/2$ nuclei have provided useful tests of empirical mass formulae whose parameters are determined from nuclei near the valley of stability. Two of the approaches which have been used are the transverse Garvey-Kelson (GK) formula [7], and the modified shell model mass equation (MSMME) by Jelley et al. [8]. In general, the MSMME has been more successful than the transverse GK in predicting the masses of the $T_z = 5/2$ sd-shell nuclei. However, difficulties with the MSMME predictions have been encountered for the lighter nuclei of this series, especially ^{19}N , where the discrepancy between the measured and predicted masses is about 500 keV for both methods. The difference between the transverse GK and MSMME predictions for the

sd-shell $T_z = 5/2$ nuclides is greatest for the mass of ^{15}B (1.14 MeV). Thus the new mass measurement of ^{15}B provides an excellent opportunity to further test the mass predictions.

The experiment was performed with a 102 MeV $^{18}\text{O}^{8+}$ beam from the Heidelberg MP tandem incident on an isotopically enriched ^{48}Ca target of about $60 \mu\text{g}/\text{cm}^2$ evaporated onto a thin carbon backing. Reaction products were momentum analyzed by a Q3D magnetic spectrograph [9] and detected by a 1.4 m long focal plane gas proportional counter detector telescope [10]. Three separated detector regions were utilized. The first two regions provided ΔE and E signals as well as position information, while the third counter section provided a veto signal for particles of long range. Four parameters consisting of ΔE , E , and the two position signals were event-mode recorded on magnetic tape. During off-line analysis, windows were set on these four parameters to separate the numerous particle groups that were simultaneously incident on the detector.

Preliminary measurements were performed at $\theta_{\text{lab}} = 8^\circ$, but the observed yield for the transition to the ground state of ^{51}V was quite small. Thus, to increase the yield, further measurements were performed with the spectrograph centered at 0° with a circular stainless steel Faraday cup, 25 mm in diameter, placed at the entrance to the spectrograph to intercept the primary beam. With the Faraday cup in place, the effective scattering angle was 2.6° and the solid angle was 8.5 msr. The high counting rate in the detector

¹ On leave from Panjab University, Chandigarh, India. Present address: LAMPF, Los Alamos, NM 87545, USA.

² Present address: BBC, Mannheim, West Germany.

³ Permanent address: Cyclotron Laboratory, Michigan State University, East Lansing, MI 48824, USA. Research partially supported by the U.S. National Science Foundation.

⁴ A.P. Sloan Fellow (1976-1978). Permanent address: Cyclotron Institute, Texas A & M University, College Station, TX 77843, USA.

NUCLEON TUNNELLING MODEL OF MASS DIFFUSION IN DEEP INELASTIC HEAVY ION COLLISIONS*

C.M. KO, G.F. BERTSCH and D. CHA

Department of Physics and Cyclotron Laboratory, Michigan State University, East Lansing, MI 48824, USA

Received 24 April 1978

Revised manuscript received 7 June 1978

We derive a simple expression for the mass diffusion coefficient in deep inelastic collisions, based on a proximity formulation of nucleon tunnelling. The predicted value of the coefficient is consistent with empirical data. The mass diffusion coefficient has a negligible dependence on excitation energy in the physically interesting domain.

Deep inelastic collisions between heavy ions occur at incident energies well above the Coulomb barrier. Besides the large cross section for energy damped events, these collisions are also characterized by many nucleons exchanged between the two ions. These latter features are evidenced by the broad mass distribution of the final fragments. Models for describing these phenomena are based on diffusion. In a simple model used by Norenberg [1] and Moretto et al. [2], the nucleon diffusion is assumed to occur when the two ions are in contact and rotating about each other; the dependence of the diffusion rate on the relative separation of the ions is treated discontinuously. Diffusion coefficients have also been extracted from the experimental data with this model by Schröder et al. [3], Sventek et al. [4] and Wolschin et al. [5]. A typical value for the empirical mass diffusion coefficient is

$$D_A \sim 10^{22} \text{ nucleon}^2/\text{s},$$

and it tends to increase as the combined system becomes heavier.

Determination of the mass diffusion coefficient from a microscopic model has been attempted by Ayik et al. [6], and by Randrup [7]. We shall use a proximity function to approximate the mass flux, as does Randrup. Unlike Randrup, we calculate the flux from the quantum

mechanical barrier penetration, rather than from a Thomas-Fermi approximation. There are no free parameters in the model, and furthermore the dependence of the diffusion coefficient on the relative separation of the two ions is also determined from the model. The dependence on separation is needed in more detailed descriptions of the reaction, such as used by Agassi et al. [8] and Schröder et al. [9].

We assume that the deep inelastic collision is peripheral and fast so that the sudden approximation is valid. This assumption has been made by most people in the field except the work of Mustafa [10]. For simplicity, we consider only a one-dimensional geometry neglecting completely the effect of angular momentum. We describe the two ions by the Fermi gas model and neglect the single-particle Coulomb potential. We take the average single-particle potential as a Woods-Saxon well characterized by the three parameters: depth V_0 , radius R , and thickness a . Then the combined potential felt by the nucleons, when the two ions are separated by the distance s measured between the half potential points, is given by

$$V(x, s) = V_0 \frac{V_0}{1 + \exp[(|x + R_1 + 0.5s| - R_1)/a]} \frac{V_0}{1 + \exp[(|x - R_2 - 0.5s| - R_2)/a]}. \quad (1)$$

This model is only applicable for $s \geq 0$. When $s < 0$, the

* Work supported by the National Science Foundation, under Grant No. PHY76-20097 A01.

Core polarization in inelastic scattering*

F. Petrovich†

Lawrence Berkeley Laboratory, University of California, Berkeley, California 94720

H. McManus, J. Borysowicz, and G. R. Hammerstein

Cyclotron Laboratory and Physics Department, Michigan State University, East Lansing, Michigan 48823

(Received 24 November 1976)

Inelastic scattering is a source of much useful information about core polarization effects in nuclei near closed shells. Although there have been many theoretical treatments of core polarization effects reported in the literature, the results of these calculations have rarely been applied to the interpretation of inelastic scattering data. In the present paper we review the microscopic models for the treatment of inelastic proton and electron scattering and the microscopic models for the treatment of core polarization. Estimates are made of core excited admixtures in the wave functions for low-lying states in ^{42}Ca , ^{50}Ti , ^{89}Y , ^{90}Zr , ^{207}Pb , and ^{209}Bi . The resulting wave functions are used to calculate theoretical (p, p') cross sections and (e, e') form factors for comparison with available experimental data. "Realistic" G matrix interactions are used as the starting point in both the structure and the (p, p') calculations. In the structure calculations the interaction is modified by means of a "bootstrap" prescription to account for important long-range core correlations and in the (p, p') calculations it is modified by the addition of an imaginary component. It is concluded that the overall features of the experimental data can be understood from these calculations.

[NUCLEAR STRUCTURE, NUCLEAR REACTIONS (p, p') and (e, e') ; nuclei near closed shells; microscopic model for core polarization; calculated $\sigma(\theta)$ and $F(q)$.]

I. INTRODUCTION

The concept of core polarization is quite well known in the shell model interpretation of nuclei in the vicinity of closed shells. In the shell model a nuclear state is described in a restricted configuration space which presumably contains the bulk of its wave function, but not all its significant components. This restricted configuration space, commonly called the model space, usually consists of a few valence particles (holes) distributed among a small number of shell model orbitals outside (inside) an inert closed shell core. The term core polarization is generally associated with effects which are due to wave function admixtures not in the model space. The name arises because these admixtures most often will consist of core-excited configurations. Core polarization can be taken into account by defining effective operators in the model space which may be calculated by means of perturbation theory.

These ideas first appeared in the literature about 20 years ago^{1,2} when it was first noted that there were discrepancies between the predictions of the simple shell model and the experimental values for nuclear magnetic moments, quadrupole moments, γ -transition rates, etc. Two different models were proposed at this time. One is a hybrid model in which the core is treated as a liquid drop which can be set into oscillation by interaction with the extracore nucleons.¹ The other is a

completely microscopic model² in which the core is considered to be an assemblage of nucleons—any of which might be raised to higher, unoccupied levels as a result of the two-body forces which couple them to the valence nucleons.

In recent times this microscopic model has been pursued in considerably greater depth. The major impetus here has been the work of Brown and collaborators³⁻⁸ whose purpose was to gain an understanding of the properties of finite nuclei using "realistic" forces, i.e., interactions which can be derived directly from the free two-nucleon potential. As the nucleon-nucleon interaction is strong and singular, the first step in this approach is to truncate to a large shell model basis by applying Brueckner Hartree-Fock theory to get rid of the short range two-nucleon correlations and replace the singular interaction by a smooth well-behaved one, namely, the bare G matrix. The second step is to truncate to the model space and to renormalize the bare G matrix to account for core polarization as described in the first paragraph above. The renormalized G matrix is the shell model effective interaction.

Kuo and Brown^{4,8} have made a systematic study of nuclei with ^{16}O , ^{40}Ca , ^{48}Ca , ^{56}Ni , ^{88}Sr , and ^{208}Pb cores using second order perturbation theory in renormalizing the bare G matrix. They find that core polarization gives rise to a strong pairing effect which is the major feature of the observed spectra. Although the results of these

$^{40}\text{Ar}(p, d)^{39}\text{Ar}$ reaction at $E_p = 35 \text{ MeV}^\dagger$

J. F. Tonn* and R. E. Segel

*Argonne National Laboratory, Argonne, Illinois 60439
and Northwestern University, Evanston, Illinois 60201*

J. A. Nolen and W. S. Chien

*Cyclotron Laboratory, Michigan State University, East Lansing, Michigan 48824*P. T. Debevec[†]*Argonne National Laboratory, Argonne, Illinois 60439*

(Received 25 April 1977)

The $^{40}\text{Ar}(p, d)^{39}\text{Ar}$ reaction has been studied at a bombarding energy of 35 MeV. A thin planar gas cell target allowed an energy resolution of 30 keV to be achieved. Excitation energies of levels in ^{39}Ar up to 5.6 MeV were obtained, angular distributions being taken from 6° to 40° (laboratory). Distorted-wave Born approximation fits were made to the observed angular distributions of the stronger states and spectroscopic factors extracted. The results are compared with previous experiments and to shell-model calculations. The data support the contention that much of the antianalog state strength is contained in the 3.379 MeV state.

[NUCLEAR REACTIONS $^{40}\text{Ar}(p, d)$, $E_p = 35 \text{ MeV}$, $\Delta E = 30 \text{ keV}$, measured $\sigma(E_d, \theta)$; DWBA analysis, deduced l values and spectroscopic factors. Planar gas cell target.]

I. INTRODUCTION

In a weak coupling picture nuclei in the mass 40 region are described in terms of a small number of particles and holes about a closed ^{40}Ca core. A good nucleus in which to quantitatively test the validity of this picture is ^{39}Ar which has 18 protons and 21 neutrons and is accessible in a variety of nuclear reactions. In other nuclei in the ^{40}Ca region a weak coupling model has had considerable success, although there is at least one significant failure: The energies of multiparticle multihole states of unstretched isospin (i.e., $T < T_p + T_n$) are found to be about 2 MeV higher than what is predicted using empirical interactions.¹⁻³ In the previously reported $^{40}\text{Ar}(p, d)$ study of Johnson and Griffiths⁴ the energy resolution was 120 keV and therefore many of the states above 2.5 MeV could not be resolved. Furthermore, Johnson and Griffiths found an anomalously low spectroscopic factor of 0.54 for the ^{39}Ar ground state. A recent shell-model calculation by Lawson and Chen⁵ yielded a more reasonable value of 1.8. The present work was therefore undertaken in order to both study the reaction with better energy resolution and also check the previously reported spectroscopic factors.

II. EXPERIMENTAL PROCEDURE AND RESULTS

The experiment was performed using a 35 MeV proton beam from the Michigan State University cyclotron. The target was a planar gas cell 0.75

mm thick with 0.0127 mm Mylar windows, filled with natural argon (99.50% ^{40}Ar). The outgoing deuterons were detected by a high resolution position sensitive proportional counter⁶ mounted in the focal plane of an Enge split pole magnetic spectrograph.

The overall energy resolution of 28 keV was limited primarily by energy loss straggling in the gas cell windows. Blistering of the gas cell windows was found to cause the resolution to deteriorate with time. Windows other than Mylar, such as thin nickel or Havar, could not be used because the less negative (p, d) Q values on such windows would cause background in the deuteron energy range of interest. By limiting gas cell pressures to 110 Torr and beam currents to 100 nA a cell could withstand about two millicoulombs of integrated beam before the resolution increased to 35 keV, at which time the gas cell was replaced with a fresh one.

Although the gas cell was changed at intervals, the blistering of the Mylar windows after exposure to the beam was still severe enough to change the cell's thickness and affect the normalization. For this reason the data were normalized for the strong states at 1.27, 1.52, and 2.36 MeV to spectra taken with a thicker gas cell. The thicker gas cell, 2.7 mm in thickness with 0.0254 Mylar windows, gave a resolution of 50 keV and showed stable yields over long periods.

Spectra were taken at angles from 6° to 40° (lab) with the thin cell, and from 6° to 55° (lab) with the

Levels of $^{16}\text{F}^\dagger$

H. Nann, W. Benenson, E. Kashy, H. P. Morsch,* and D. Mueller[†]

Cyclotron Laboratory and Department of Physics, Michigan State University, East Lansing, Michigan 48824

(Received 8 March 1977)

Levels of ^{16}F have been investigated by means of the $^{19}\text{F}(^3\text{He}, ^6\text{He})$ reaction at 70 MeV bombarding energy and the $^{16}\text{O}(^3\text{He}, t)$ reaction at 35 MeV. Three new states at 4.71, 6.05, and 6.93 MeV have been found.

[NUCLEAR REACTIONS $^{19}\text{F}(^3\text{He}, ^6\text{He})$, $E_{^3\text{He}} = 70$ MeV, $^{16}\text{O}(^3\text{He}, t)$, $E_{^3\text{He}} = 35$ MeV.]
 ^{16}F deduced levels.

In the past there has been considerable interest in the structure of the $A=16$, $T=1$ isobaric triplet. Among these nuclei, ^{16}F is the least studied since it can be reached only by a few reactions.¹⁻⁴ We have studied the $^{19}\text{F}(^3\text{He}, ^6\text{He})^{16}\text{F}$ and $^{16}\text{O}(^3\text{He}, t)^{16}\text{F}$ reactions with the aim of obtaining additional information about the level structure of ^{16}F .

The two experiments were performed with 70 and 35 MeV ^3He -particle beams from the Michigan State University cyclotron. The reaction products were detected in the focal plane of an Enge split-pole spectrograph with a position sensitive proportional counter. The proportional counter was backed by a scintillation counter which was run in coincidence with it to provide particle identification by measuring the time of flight through the spectrograph. As targets, CaF_2 evaporated onto a thin carbon backing and a Mylar foil were used. For the $^{19}\text{F}(^3\text{He}, ^6\text{He})$ reaction, angles of 7° , 9° ,

and 12° were employed, whereas the $^{16}\text{O}(^3\text{He}, t)$ reaction was measured at 9° and 12° . The spectra from the $^{19}\text{F}(^3\text{He}, ^6\text{He})$ reaction were calibrated by means of the $^{13}\text{C}(^3\text{He}, \alpha)^{12}\text{C}$ and $^{19}\text{F}(^3\text{He}, \alpha)^{18}\text{F}$ reactions. For the $^{16}\text{O}(^3\text{He}, t)$ reaction, the contaminant peaks from the $^{12}\text{C}(^3\text{He}, t)$ reaction served as calibration by sweeping them across the detector. Figure 1 shows a ^6He spectrum from the $^{19}\text{F}(^3\text{He}, ^6\text{He})$ reaction, whereas in Fig. 2 a triton spectrum from the $^{16}\text{O}(^3\text{He}, t)$ reaction is displayed. The energy resolution in the $(^3\text{He}, ^6\text{He})$ experiment was about 80 keV and in the $(^3\text{He}, t)$ experiment about 60 keV. Three new states which were found in ^{16}F via the $^{19}\text{F}(^3\text{He}, ^6\text{He})$ reaction are marked by an asterisk in Fig. 1.

TABLE I. Results of the $^{19}\text{F}(^3\text{He}, ^6\text{He})$ and $^{16}\text{O}(^3\text{He}, t)$ reactions. E_x is accurate within ± 20 keV.

Present work		Reference 1	
$^{19}\text{F}(^3\text{He}, ^6\text{He})$	$^{16}\text{O}(^3\text{He}, t)$	$^{14}\text{N}(^3\text{He}, n)$	L
E_x (MeV)	E_x (MeV)	E_x (MeV)	
0	0	0	1
0.19	0.19	0.192	1
0.42	0.43	0.425	3
0.72	0.72	0.722	(3)
3.75	3.75	3.751	0
3.86	3.86	3.861	2
4.37	4.37	4.370	
4.66	4.66	4.646	0
4.71			
4.97		4.973	2
		5.264	
5.39		5.390	2
		5.448	
5.53	5.53	5.528	2
		5.840	
6.05			
		6.230	
		6.371	
6.68	6.68	6.678	
6.93			

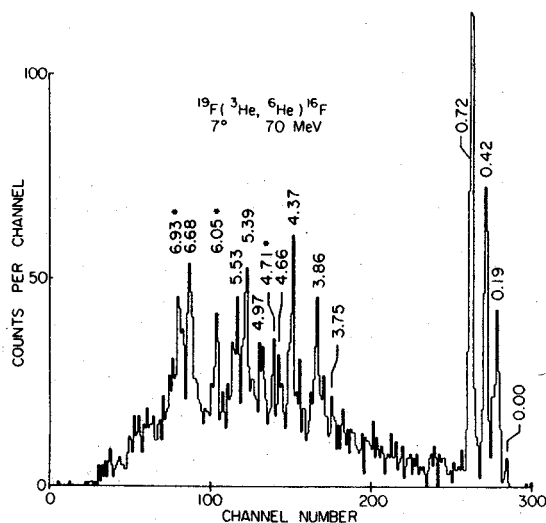


FIG. 1. Spectrum from the $^{19}\text{F}(^3\text{He}, ^6\text{He})^{16}\text{F}$ reaction. The states are labeled by their excitation energy. New states are marked by an asterisk.

${}^7\text{Li}$ and ${}^7\text{Be}$ production in the $\alpha + \alpha$ reaction*C. H. King, Sam M. Austin, H. H. Rossner,[†] and W. S. Chien*Cyclotron Laboratory and Physics Department, Michigan State University, East Lansing, Michigan 48824*

(Received 20 June 1977)

Differential cross sections for the ${}^4\text{He}(\alpha, p)$ reaction leading to the ground and 478-keV states of ${}^7\text{Li}$ have been measured at 11 energies between 39.0 and 49.5 MeV and used to determine integral cross sections for ${}^7\text{Li}$ production in ${}^4\text{He}(\alpha, p)$. Comparison of the ground state cross sections with ${}^7\text{Li}(p, \alpha)$ data using the principle of detailed balance indicates good agreement with the most recent ${}^7\text{Li}(p, \alpha)$ measurements but not with some older results. Cross sections for ${}^4\text{He}(\alpha, d){}^6\text{Li}$ (ground state), extracted at three energies, are consistent with the most recent ${}^6\text{Li}(d, \alpha)$ measurements. Cross sections for ${}^7\text{Be}$ production via ${}^4\text{He}(\alpha, n){}^7\text{Be}$ were determined at nine energies between 39.4 and 47.4 MeV by direct collection of the ${}^7\text{Be}$ and detection of the γ rays following its decay. These cross sections are essentially identical to the ${}^7\text{Li}$ production cross sections above 43 MeV but are smaller below this energy because of threshold effects. The ${}^4\text{He}(\alpha, p)$ and ${}^4\text{He}(\alpha, n)$ reactions are involved in several mechanisms which have been proposed to explain the universal abundance of ${}^7\text{Li}$, and calculations of these processes have assumed cross sections larger than our data. We therefore confirm earlier conclusions that ${}^7\text{Li}$ is unlikely to be produced by galactic cosmic-ray spallation alone, but the status of the other mechanisms remains unclear. Peaks in the ${}^4\text{He}(\alpha, p)$ and ${}^4\text{He}(\alpha, n)$ excitation functions are discussed in terms of resonances in ${}^8\text{Be}$. Parameters determined by Kumar and Barker in a fit to ${}^7\text{Li}(p, \alpha)$ data are inadequate to explain our ${}^4\text{He}(\alpha, p){}^7\text{Li}$ (478 keV) cross sections.

NUCLEAR REACTIONS ${}^4\text{He}(\alpha, p)$, $E = 39.0\text{--}49.5$ MeV; measured $\sigma(E; \theta, E_p)$, $\sigma(E)$. ${}^4\text{He}(\alpha, n)$, $E = 39.4\text{--}47.4$ MeV; measured $\sigma(E)$. ${}^4\text{He}(\alpha, d)$, $E = 46.7\text{--}49.5$ MeV; measured $\sigma(E; \theta)$, $\sigma(E)$. Astrophysical implications for ${}^7\text{Li}$ production considered. Discussion of ${}^8\text{Be}$ levels in R -matrix formalism.

I. INTRODUCTION

The observed abundances of the nuclides with $A \geq 12$ can be explained remarkably well by assuming that they were created through chains of nuclear reactions in stellar interiors.¹ However, creation of the lighter nuclides seems to require for the most part an alternative mechanism: This is particularly true of deuterium and the isotopes of lithium, beryllium and boron, which are too fragile to survive in the hot environment of stellar interiors. Although the abundance of these nuclides is very low, the explanation of their origin can have significant consequences for our understanding of the universe. For example, in the case of deuterium it appears that no realistic process other than a primordial big bang can produce this nuclide in sufficient amounts to explain the observed abundance.² This result implies that most of the deuterium in the universe is of cosmological origin,^{2,3} a conclusion which suggests that the universe is open.

A likely mechanism for the creation of several of the light elements is the spallation of interstellar matter by cosmic rays. Calculations of the production rates in this process indicate that ${}^6\text{Li}$ and the stable beryllium and boron isotopes can be produced in approximately sufficient amounts. However, ${}^7\text{Li}$ appears to be significantly underproduced,^{4,5} although the calculations for this isotope contain substantial uncertainties. Since significant amounts of ${}^7\text{Li}$ can also be created in a big bang,³ the abundance of this isotope might provide an additional constraint on the nature of the universe if non-cosmological mechanisms should prove insufficient.

The principal source of ${}^7\text{Li}$ in cosmic-ray spallation is the interaction between ${}^4\text{He}$ in cosmic rays and ${}^4\text{He}$ in the interstellar medium. This interaction can produce ${}^7\text{Li}$ directly via the ${}^4\text{He}(\alpha, p)$ reaction to one of the two

particle-stable states of ${}^7\text{Li}$: the ground state and the first excited state (478 keV). In addition, since ${}^7\text{Be}$ decays to ${}^7\text{Li}$ by electron capture, the reaction ${}^4\text{He}(\alpha, n)$ to the two analogous states in ${}^7\text{Be}$ (ground state and 429 keV state) also contributes to the net production of ${}^7\text{Li}$. Until recently very few direct measurements of the cross sections in these four channels were available. Instead, in the spallation calculations,^{4,5} the cross sections for the ${}^4\text{He}(\alpha, p)$ reaction to the ${}^7\text{Li}$ ground state were inferred by detailed balance from measured ${}^7\text{Li}(p, \alpha)$ cross sections. Assumptions were then made about the cross sections in the other three channels. The uncertainty in the calculated ${}^7\text{Li}$ production was further enhanced by substantial discrepancies in measurements of the ${}^7\text{Li}(p, \alpha)$ cross sections.

Because of their potential importance for understanding the origin of ${}^7\text{Li}$, we have measured the relevant $\alpha + \alpha$ cross sections for α energies from just above threshold (34.7 MeV for ${}^4\text{He}(\alpha, p)$ and 38.0 MeV for ${}^4\text{He}(\alpha, n)$) up to 50 MeV. This energy region is particularly important, since the cross sections are largest at these low energies, and some models for cosmic-ray spallation⁴ assume the cosmic-ray flux to be large at low energies as well. Other mechanisms which have been proposed for ${}^7\text{Li}$ production (considered in Sec. IV B) are also sensitive to the low-energy $\alpha + \alpha$ cross sections. The experimental procedure and data reduction for the ${}^4\text{He}(\alpha, p)$ reaction are described in Sec. II of this paper and those for the ${}^4\text{He}(\alpha, n)$ reaction in Sec. III. The possible astrophysical implications of these measurements are discussed in Sec. IV. In the energy range covered by the present experiments peaks appear in the excitation functions which can be interpreted as resulting from resonances in the compound nucleus ${}^8\text{Be}$. Information obtained about the structure of ${}^8\text{Be}$ is described in Sec. V. Finally, a summary of our results and conclusions is provided in Sec. VI. A

Mass of ${}^6\text{He}$

R. G. H. Robertson, E. Kashy, W. Benenson, and A. Ledebuhr

Cyclotron Laboratory and Department of Physics, Michigan State University, East Lansing, Michigan 48824

(Received 4 August 1977)

A precise value for the ${}^6\text{He}$ mass excess has been obtained by comparison of the Q values for the ${}^7\text{Li}(d, {}^3\text{He}){}^6\text{He}$ and ${}^{19}\text{F}(d, {}^3\text{He}){}^{18}\text{O}^*$ reactions, the latter populating the first excited state of ${}^{18}\text{O}$. The measurements were performed at 0° in a magnetic spectrograph. The result for the ${}^6\text{He}$ mass excess is (17593.7 ± 1.1) keV, about 3 keV less than the previous value, and 3 times more accurate. The effect on the $A = 8$ isobaric quintet and on the β decay of ${}^6\text{He}$ is discussed.

[NUCLEAR REACTIONS ${}^7\text{Li}(d, {}^3\text{He}){}^6\text{He}$, ${}^{19}\text{F}(d, {}^3\text{He}){}^{18}\text{O}$. $E_d = 20.8$ MeV, $\theta = 0^\circ$,
magnetic spectrograph. ${}^6\text{He}$, measured mass excess.]

I. INTRODUCTION

With the exception of ${}^6\text{He}$, the masses of all the light nuclei near the line of stability have been measured to a precision of the order of 1 keV or better. The mass of ${}^6\text{He}$ was measured in 1963 by Johnson, Pleasonton and Carlson¹, who examined the energy spectrum of ${}^6\text{Li}$ recoils following the β^- decay of ${}^6\text{He}$ and obtained a value for the decay energy accurate to 4 keV. No other measurement has approached that accuracy.

The ${}^6\text{He}$ mass is important in two respects. First, ${}^6\text{He}$ is a product of many reactions which lead to nuclei far from the line of stability², or serves in auxiliary calibration reactions³, and its mass is becoming a limiting factor in the precision of some measurements of that type. Second, the ${}^6\text{He}$ β decay is the fastest Gamow-Teller transition, and as such has received much attention in investigations of the renormalization of the axial-vector coupling constant in nuclear matter^{4,5}. An accurate determination of the ft value for the decay depends on precise knowledge of the ${}^6\text{He}$ - ${}^6\text{Li}$ mass difference.

The present paper reports a measurement of the ${}^6\text{He}$ mass based on a comparison of the Q -values for the ${}^7\text{Li}(d, {}^3\text{He}){}^6\text{He}$ and the ${}^{19}\text{F}(d, {}^3\text{He}){}^{18}\text{O}^*$ reactions, the latter populating the first excited state of ${}^{18}\text{O}$ at 1.982 MeV.

II. EXPERIMENTAL METHOD AND RESULTS

In general the comparison of two nuclear reactions as a means of measuring a mass is subject to uncertainties arising from a number of sources, among which are: (a) imperfect knowledge of, and random variation in, the beam energy, (b) uncertainties in detector calibration and stability, (c) target thickness and the distribution of constituents throughout the target, and, (d) errors in the reaction angle. These effects have been minimized in this work by an appropriate choice of reactions and experimental conditions.

The method consisted of bombarding a natural LiF target with 20.8 MeV deuterons from the Michigan State University Cyclotron and observing outgoing ${}^3\text{He}$ particles in the focal plane of an Enge split-pole spectrograph. Groups from the $(d, {}^3\text{He})$ reaction populating the ground state of ${}^6\text{He}$ and the first excited state of ${}^{18}\text{O}$ fell very close together (less than 30 keV apart) in the focal plane. Under these conditions the influence of the beam energy is negligible, and focal plane calibration to the required precision is straightforward. Use of a LiF target confers

the advantages of a stable binary compound. Finally, to obviate the need to measure and control the reaction angle, the experiment was performed at 0° , with the beam being stopped in a Faraday cup located between the first and second poles of the magnet.

Reaction products were detected on the focal plane, in a resistive-wire, charge-division proportional counter of length 20 cm backed by a plastic scintillator for particle identification. The experimental procedure was to cycle the spectrograph magnet and then record ${}^3\text{He}$ spectra at a series of increasing spectrograph fields which moved the ${}^6\text{He}$ - ${}^{18}\text{O}^*$ doublet along the length of the detector. Knowledge of the spectrograph calibration⁶ permitted the detector calibration to be determined, and the doublet separation could then be extracted with high precision. The detector calibration was assumed to be linear over small distances. The principal uncertainty is the possible occurrence of small-scale nonlinearities in the detector (due for example to microscopic variations in wire diameter, dust on the wire, etc.), and such variations are presumed to average out in a set of measurements made at several locations on the detector.

Data were taken in groups of two to four consecutive field settings. Energy resolution ranged from 12 to 20 keV, depending on target thickness and beam conditions, and the doublet was not always completely resolved. Therefore, the doublet separation was derived by use of the peak-fitting code SAMPO,⁷ which gave results in good agreement with direct centroid determination in those cases for which the peaks were well resolved. One of the doublet measurements, with the fitted shape, is shown in Fig. 1. The energy resolution is approximately 15 keV full width at half maximum in that spectrum. In all, fourteen measurements were taken, eleven with a $25 \mu\text{g cm}^{-2}$ LiF target on a $20 \mu\text{g cm}^{-2}$ carbon backing, with the LiF side facing the spectrograph. One measurement was made with the target reversed and two with an $8 \mu\text{g cm}^{-2}$ target. The results are shown in Fig. 2. The data comprise a measurement of the quantity $Q_6 - Q_{18}^*$, where Q_6 and Q_{18}^* are the Q -values of the ${}^7\text{Li}(d, {}^3\text{He}){}^6\text{He}$ and ${}^{19}\text{F}(d, {}^3\text{He}){}^{18}\text{O}(1.98216)$ reactions, respectively. However, to make a comparison between the present measurement and the previous one, the ordinate of Fig. 2 is the quantity

$$\Delta = Q_6 - Q_{18}^* - (Q_6 - Q_{18}^*)_{1971},$$

where the last term is the Q -value difference that would be calculated using the 1971 mass table of Wapstra and Gove⁸ (wherein the ${}^6\text{He}$ mass is essentially based on the

Decay of $^{143}\text{Gd}^{m+g}$ by positron emission and electron capture*

R. B. Firestone, R. A. Warner, and Wm. C. McHarris

Department of Chemistry, Cyclotron Laboratory, and Department of Physics

W. H. Kelly

Cyclotron Laboratory and Department of Physics, Michigan State University, East Lansing, Michigan 48824

(Received 3 August 1977)

In this study the decay of $^{143}\text{Gd}^{g+m}$ by positron emission and electron capture and the isomeric decay of $^{143}\text{Eu}^m$ were investigated. γ rays associated with $^{143}\text{Gd}^{g+m}$ were placed on the basis of excitation functions, half-life, and γ - γ coincidence information. We assigned 61 γ rays deexciting 33 levels in ^{143}Eu from the decay of 112 ± 2 sec $^{143}\text{Gd}^m$. Another 7 γ rays deexcite an additional 6 levels in ^{143}Eu from 39 ± 2 sec $^{143}\text{Gd}^g$ decay. A small delayed p or α branch associated with ^{143}Gd decay was observed with an upper limit of 1×10^{-5} . The half-life of the $^{143}\text{Eu}^m$ isomer at 389.47 keV was found to be 50.0 ± 0.5 μ sec. The resulting level structure observed in ^{143}Eu is explained quite satisfactorily in terms of a triaxial weak-coupling model.

<p>RADIOACTIVITY $^{143}\text{Gd}^{g+m}$, $^{143}\text{Eu}^m$, measured $T_{1/2}$, delayed $p + \alpha$, E_γ, I_γ, $\gamma\gamma$ coin, $\sigma(E)$; deduced $\log ft$, Q. ^{143}Eu deduced levels, J, π.</p> <p>NUCLEAR STRUCTURE ^{143}Eu; calculated levels, J, π. Triaxial weak-coupling model.</p>

I. INTRODUCTION

The decay of $^{143}\text{Gd}^{g+m}$ continues our studies of odd-mass $N=79$ nuclei, which have included $^{137}\text{Ce}^{g+m}$,¹ $^{139}\text{Nd}^{g+m}$,² and $^{141}\text{Sm}^{g+m}$.^{3,4} The first studies of $^{143}\text{Gd}^m$ decay were reported by J. van Klinken et al.,⁵ who presented a modest decay scheme; later studies, by Wisshak et al.,⁶ presented a more thorough decay scheme. In this work we have nearly doubled the known information about $^{143}\text{Gd}^m$ decay and present our new data concerning $^{143}\text{Gd}^g$ decay. We had previously reported a half-life measurement of $^{143}\text{Gd}^{g+m}$;⁷ here we present our total decay scheme data in more detail. The level structure in ^{143}Eu was discussed by Wisshak et al. in terms of a generalized decoupling model, which gave only fair agreement with experiment. In this paper we shall show that a good qualitative agreement with experiment can be attained using a weak-coupling model.

II. SOURCE PREPARATION

$^{143}\text{Gd}^{g+m}$ were produced by the $^{144}\text{Sm}(^3\text{He}, 4n)^{143}\text{Gd}$ reaction with a 50-MeV ^3He beam produced by the Michigan State University sector-focused cyclotron. Enriched targets of $^{144}\text{Sm}_2\text{O}_3$ (95.10% ^{144}Sm , obtained from the Isotopes Division, Oak Ridge National Laboratory) were bombarded in the terminal of a He-jet recoil transport system, which is described elsewhere.⁷ The primary impurities encountered in these studies were ^{140}Pm ($t_{1/2} = 5.8$ min), $^{141}\text{Sm}^m$ ($t_{1/2} = 22.7$ min), ^{142}Eu ($t_{1/2} = 1.2$ min), ^{144}Eu ($t_{1/2} = 10.5$ sec), ^{140}Gd ($t_{1/2} = 70.5$ sec), ^{146}N ($t_{1/2} = 7.11$ sec), ^{10}C ($t_{1/2} = 19.4$ sec), and the ^{143}Eu daugh-

ter activity ($t_{1/2} = 2.61$ min). None of these impurities was both intense and complex enough to hinder the studies of interest seriously, and all were already well understood. Coincidence and half-life experiments were employed to delineate the transitions of interest further.

III. γ -RAY SPECTRA

A. Singles spectra

$^{143}\text{Gd}^{g+m}$ singles spectra were taken with an 18.0% efficient Ge(Li) detector (relative to a 7.6 \times 7.6-cm NaI(Tl) detector at 25 cm for the 1332-keV ^{60}Co photopeak). The resolution of this detector was 2.1 keV full width at half maximum at 1332 keV. Activity was collected on a slowly moving paper tape at a point shielded from the detector and counted during the interval from 10 sec to 90 sec after bombardment. A spectrum collected in this manner is shown in Fig. 1.

Seven γ rays were assigned to $^{143}\text{Gd}^g$ decay and 61 γ rays were assigned to $^{143}\text{Gd}^m$ decay; these are listed in Table I. Assignments were made on the basis of half-life, excitation functions, and coincidence information (discussed below), and virtually all of the observed activity could be assigned either to $^{143}\text{Gd}^{g+m}$ or to the appropriate known impurity. Precise energy calibrations were performed using ^{56}Co , $^{110}\text{Ag}^m$, ^{152}Eu , ^{182}Ta , and ^{226}Ra internal standards, and the quoted errors reflect the statistical scatter in these measurements. Certain transitions were apparent only in the coincidence studies, and greater errors are reflected in these energy and intensity assignments.

The paper of Wisshak et al.⁶ included

Mass of ^{21}O from the $^{18}\text{O}(^{18}\text{O}, ^{15}\text{O})^{21}\text{O}$ reaction

F. Naulin, C. Détraz, M. Bernas, E. Kashy,* M. Langevin, F. Pougheon, and P. Roussel

Institut de Physique Nucléaire, BP No. 1, 91406 Orsay, France

(Received 22 September 1977)

The mass of ^{21}O is measured as 8.153 ± 0.070 MeV from the Q value of the $^{18}\text{O}(^{18}\text{O}, ^{15}\text{O})^{21}\text{O}$ reaction at 91 MeV.

[NUCLEAR REACTIONS $^{18}\text{O}(^{18}\text{O}, ^{15}\text{O})$, $E=91$ MeV; measured ^{21}O mass. Enriched target.]

The measurement of masses of nuclei far from β stability has provided a useful test of the various theoretical models and predictions, most of which have recently been compiled.¹ As one moves away from the line of stability the predictions tend to diverge and experimental data are then essential. The predictions of masses even further from the known data are then considerably improved by inclusion of such new data. So far, there has been only one measurement of the ^{21}O mass, using the $^{208}\text{Pb}(^{18}\text{O}, ^{21}\text{O})^{205}\text{Pb}$ reaction.²

The 91 MeV $^{18}\text{O}(6^+)$ beam from the Orsay MP tandem was used to bombard an $\text{Al}_2^{18}\text{O}_3$ self-supporting target enriched to 90% ^{18}O . The target, which was prepared by anode oxidation,³ had a thickness of $130 \mu\text{g}/\text{cm}^2$ and showed no apparent damage under bombardment of a 400 nA ^{18}O beam. The emitted nuclei were analyzed in a 180° magnetic spectrograph with a solid angle of 3×10^{-3} sr, and detected in the magnetic focal plane by a counter telescope consisting of two ΔE gas-filled resistive-wire proportional counters backed by 10 cm long silicon detectors which measured both position and total energy of the ions.

The procedure of nucleus identification has been described elsewhere.^{4,5} The energy spectra of ^{15}O were measured at 7° and 8° in the laboratory. Figure 1(a) shows the 8° spectrum of ^{15}O for the $^{18}\text{O}(^{18}\text{O}, ^{15}\text{O})^{21}\text{O}$ reaction. The background in Fig. 1(a), with a cross section of $25 \mu\text{b sr}^{-1} \text{MeV}^{-1}$ is mostly due to the $(^{18}\text{O}, ^{15}\text{O})$ reaction on ^{27}Al which populates states in ^{30}Al between 7.5 and 10.5 MeV excitation energies. There is also an indication of some contribution from the $^{16}\text{O}(^{18}\text{O}, ^{15}\text{O})^{19}\text{O}$ reaction. Figure 1(b) shows the ^{15}O spectrum from the bombardment of an $\text{Al}_2^{16}\text{O}_3$ target, which was used to check for the contributions from ^{27}Al and ^{16}O .

The only peak identified as corresponding to an ^{21}O state corresponds to a mass excess of 8.153 ± 0.070 MeV for that state, in good agreement with the recently reported value² of 8.122 ± 0.075 MeV

for the ^{21}O ground state. Combining these results, we obtain a mass excess of 8.138 ± 0.50 MeV.

As discussed elsewhere,⁴ the uncertainty of our experimental value has two main origins. One bears on the position of the peak centroid in the spectrum of Fig. 1(a). The second arises from the calibration of the magnetic rigidity of the detected nucleus versus the electronically measured position in the focal plane. As long as the nucleus is detected in the kinematically corrected focal plane, as was done for ^{15}O , no sizable uncertainty arises from the finite angular aperture. But most calibrating transitions, such as those from $^{18}\text{O}(^{18}\text{O}, ^{20}\text{Ne})^{16}\text{C}$, have a different kinematic correction, which leads to an angular dependent broadening of the experimental peak. That major source of uncertainty was reduced by using a horizontal aperture of 0.25° for the calibrating transition instead of the 4° aperture used for ^{15}O .

The comparison of the ^{21}O mass with predictions is shown in Table I. ^{21}O is seen to be significantly more bound than expected by these predictions. Finally, the strong background caused by ^{27}Al and the apparent weakness of their cross section prevented the observation of the predicted⁷ excited levels of ^{21}O which we had hoped to make when the measurement was undertaken.

TABLE I. ^{21}O mass excess (MeV).

Groote, Hilf, and Takahashi ^a	8.43
Liran and Zeldes ^a	9.43
Janecke, Garvey, and Kelson ^a	9.02
Comay and Kelson ^a	8.79 ± 0.19
Jelley <i>et al.</i> ^b	8.39
Experimental value ^c	8.138 ± 0.050

^aReference 1, p. 478.^bReference 6.^cReference 2 and present result, combined value.

Inelastic scattering of 40 MeV protons from ^{24}Mg . I. Natural parity transitions*

B. Zwieglinski,† G. M. Crawley, H. Nann, and J. A. Nolen, Jr.
Cyclotron Laboratory, Michigan State University, East Lansing, Michigan 48824
 (Received 15 August 1977)

Angular distributions for the inelastic scattering of protons from ^{24}Mg have been measured at a proton energy $E_p = 40$ MeV with a resolution of 16 keV. The results for the natural parity states in the excitation energy range from the ground state up to $E_x \approx 13.5$ MeV are presented. The data have been analyzed using a macroscopic collective model. Coupled-channel calculations assuming the rigid-rotor model have been performed for the ground-state rotational band in ^{24}Mg . Previous conclusions on the smallness of the parameter of the hexadecapole deformation have been confirmed. The angular distribution for the 6^+ member of the ground-state rotational band at 8.120 MeV made it possible to extract the sixth order deformation parameter. Negative values of β_6 are suggested by the data. Collective model distorted-wave Born approximation calculations were performed to determine the deformation parameters β_L and isoscalar transition rates $B(\text{IS}, 0_1^+ \rightarrow L)$ for most of the observed states. Nearly half of the strength observed below $E_x = 13.5$ MeV for the transitions of multipolarities $L = 2, 3$, and 4 is contained in the high-energy region between $E_x = 7.5$ and 13.5 MeV. Good agreement with the inelastic electron scattering data has been obtained for most of the low-energy transitions which were previously studied via (e, e') . Evidence is presented in favor of a particular spin value for a number of states for which only multiple spin assignments were previously made.

NUCLEAR REACTIONS $^{24}\text{Mg}(p, p')$, $E = 40$ MeV; measured $\sigma(E_p; \theta)$; deduced β_L 's, optical parameters. Enriched target.

I. INTRODUCTION

In the past the nucleus ^{24}Mg has been studied by inelastic scattering quite extensively.^{1,2} These studies concentrated mainly on low-lying levels because of a lack of sufficiently good energy resolution. The present high-resolution (p, p') experiment was intended to overcome this deficiency so that angular distributions for individual levels into the region of unbound levels could be measured. Depending on how stable and similar are the shapes of the angular distributions and how well they can be fitted by distorted-wave Born approximation (DWBA) calculations, multipole transition strengths can be extracted for these higher excited states and their distribution as a function of excitation energy studied. Similar goals were pursued in a recent (α, α') experiment by Yang et al.³ at 70 MeV bombarding energy and in an (e, e') experiment by Johnston and Drake⁴ at 120 MeV. The energy resolution in both these experiments was in many cases not sufficient to determine the transition strength for individual levels particularly at higher excitation energies.

The nucleus ^{24}Mg is believed⁵ to have a substantial quadrupole deformation in its ground state. The determination of β_2 , the parameter for the quadrupole deformation in the ground-state rotational band of ^{24}Mg , has been the subject of numerous experiments. However the determination of the hexadecapole deformation has been attempted in only a few cases. The most recent of these are summarized in Ref. 2. The trend of the quadrupole and the hexadecapole deformations in the lower half of the s - d shell has been determined by Rebel et al.⁶ from the study of the inelastic scattering of 104 MeV α -particles. The hexadecapole moment is found to display a minimum at the magnesium isotopes—its value is consistent with zero. This favorable condition suggests that it might therefore be possible to determine the β_6 deforma-

tion parameter of the potential distribution about which nothing is known at present for s - d shell nuclei. This requires a high-resolution experiment in order to resolve the weakly excited $K^\pi = 0^+, 6^+$ state at 8.120 MeV from the strongly excited 3^- state at 8.358 MeV. In addition, a high-resolution study of ^{24}Mg by inelastic scattering has considerable spectroscopic interest. For many states several possible spin-parity assignments have been suggested.⁷ The present experiment should help to establish unique spin assignments.

The results concerning the transitions to the natural parity $T=0$ states are the subject of the present paper. The unnatural parity states and the $T=1$ states will be discussed in a later publication. Some of the present results have been reported briefly.⁸

II. EXPERIMENTAL METHOD

The experiment was carried out using protons of energy 40.02 ± 0.02 MeV from the Michigan State University Isochronous Cyclotron. The scattered protons were detected in the focal plane of the Enge split-pole magnetic spectrometer using a 50 cm long position-sensitive proportional counter with delay-line readout.⁹ A self-supporting foil $310 \pm 20 \mu\text{g}/\text{cm}^2$ thick, enriched to 98.8% in ^{24}Mg served as a target. The data were measured relative to elastic events monitored with a NaI(Tl) detector at 90° to obtain relative angular distributions. These agreed with the cross sections obtained from the integrated charge to within 10%.

Because of the finite length of the counter and because the low lying states were generally much more intense than the states at higher excitation energy, the measurements were made in two passes. In the first series, covering the excitation energy range from the ground state up to $E_x \approx 8.5$ MeV, the angular distributions for the most intense lines in the spectrum were measured from 6°

(p, t) and $(p, {}^3\text{He})$ reactions on ${}^{39}\text{K}^\dagger$

H. Nann and B. H. Wildenthal

Cyclotron Laboratory and Department of Physics, Michigan State University, East Lansing, Michigan 48824

(Received 5 May 1977)

Angular distributions of the ${}^{39}\text{K}(p, t){}^{37}\text{K}$ and ${}^{39}\text{K}(p, {}^3\text{He}){}^{37}\text{Ar}$ reactions between 3° and 55° have been measured at 40 MeV bombarding energy. The experimental differential cross sections of the transitions to several of the low-lying mirror pairs of even-parity final states in ${}^{37}\text{K}$ and ${}^{37}\text{Ar}$ are compared to results of microscopic distorted-wave Born-approximation calculations based on current shell-model wave functions. The sensitivity of these distorted-wave Born-approximation calculations to optical model parameters is studied.

[NUCLEAR REACTIONS ${}^{39}\text{K}(p, t)$, ${}^{39}\text{K}(p, {}^3\text{He})$, $E_p = 40$ MeV; measured $\sigma(E_t, E_{\text{He}}, \theta)$; natural target; DWBA analysis.]

I. INTRODUCTION

The different selectivity of the (p, t) and $(p, {}^3\text{He})$ reactions on $T_z = \frac{1}{2}$ target nuclei leading to mirror final states can be used, in principle, to test different parts of the initial and final states wave functions. In practice, however, uncertainties in the distorted-wave Born-approximation (DWBA) calculations tend to mask the distinctive features and leave the analysis to some degree ambiguous.

The present ${}^{39}\text{K}(p, t)$ and ${}^{39}\text{K}(p, {}^3\text{He})$ work is part of a systematic investigation of the (p, t) and $(p, {}^3\text{He})$ reactions on $T_z = \frac{1}{2}$ nuclei in the $2s-1d$ shell^{1,2} with the aim of testing the two-particle correlations in current shell-model wave functions. For the initial and final nuclei several sets of shell-model wave functions exist^{3,4} which were calculated in the full $1d_{5/2}-2s_{1/2}-1d_{3/2}$ vector space. One set of calculations³ uses two-body matrix elements derived by reaction matrix techniques from the Hamada-Johnstone nucleon-nucleon scattering potential. In recent calculations⁴ the two-body matrix elements were treated as independent free parameters adjusted to fit experimental ground state binding energies and level spacings.

Based on these shell-model wave functions, DWBA calculations have been carried out and compared to the experimental data. The structure of most of the nuclear states involved is rather simple. Thus, the effects of the uncertainties in the DWBA calculations, such as optical model parameters or form factor descriptions, upon the conclusions which can be drawn about the wave functions used in the analysis can be studied.

II. EXPERIMENTAL PROCEDURE AND RESULTS

The experiments were carried out with a 40 MeV proton beam from the Michigan State University cyclotron. The reaction products were momentum

analyzed in an Enge split-pole magnetic spectrograph and detected in the focal plane with a position sensitive resistive-wire-proportional counter plastic-scintillator combination. This equipment provided excellent particle identification and an energy resolution of about 30 keV. The targets were made by evaporating natural potassium metal (93% ${}^{39}\text{K}$ and 7% ${}^{41}\text{K}$) onto thin carbon backings. These targets were kept under vacuum throughout the experiment. The target thicknesses ranged from 35 to 150 $\mu\text{g}/\text{cm}^2$. A NaI scintillation counter placed in the scattering chambers at 90° allowed continuous monitoring of the target conditions and the normalization of the relative cross sections at different angles.

The relative (p, t) to $(p, {}^3\text{He})$ cross sections were measured during the same experimental run, with the same configuration of target, beam, and detector system. Only the magnetic field of the spectrograph was changed in order to bring the triton and ${}^3\text{He}$ particles to the same position on the focal plane. The error in the relative (p, t) to $(p, {}^3\text{He})$ cross section is estimated to be less than 10%. The absolute cross section normalization for the (p, t) and $(p, {}^3\text{He})$ data was taken relative to the elastic proton scattering cross section in the angular region from 25° to 50° . Again an identical experimental configuration was used for these different measurements. The measured elastic cross sections were assumed to have the values calculated in the optical model from the parameters of Becchetti and Greenlees.⁵ The accuracy of the absolute differential cross section is estimated to be about 20%.

Figure 1 shows spectra from the ${}^{39}\text{K}(p, t){}^{37}\text{K}$ reaction in the upper half and from the ${}^{39}\text{K}(p, {}^3\text{He}){}^{37}\text{Ar}$ reaction in the lower half. Only the even parity states in the final nuclei are populated with reasonable strength. Groups due to contaminants are hatched.

Mass of lowest $T = 2$ state of ^{12}C

R. G. H. Robertson, T. L. Khoo,* and G. M. Crawley

Cyclotron Laboratory and Physics Department, Michigan State University, East Lansing, Michigan 48824

A. B. McDonald

AECL Chalk River Nuclear Laboratories, Chalk River, Ontario, Canada, K0J 1J0

E. G. Adelberger

Department of Physics, University of Washington, Seattle, Washington 98105

S. J. Freedman

Department of Physics, Stanford University, Stanford, California 94305

(Received 9 January 1978)

A precise measurement of the excitation energy of the lowest $T = 2$ state in ^{12}C has been made via the $^{14}\text{C}(p,t)^{12}\text{C}$ reaction. The value obtained, 27.5950 ± 0.0024 MeV, is in agreement with earlier (less precise) measurements and therefore does not explain the failure to observe the $T = 2$ state in isospin-forbidden resonance reactions. Also reported in this work are an upper limit of 30 keV for the total width of the $T = 2$ state and an excitation energy of 3.3492 ± 0.0012 MeV for the first excited state of ^{10}C .

NUCLEAR REACTIONS $^{14}\text{C}(p,t)$, $E_x = 27.6$ MeV, measured Q , Γ . $^{12}\text{C}(p,t)$, $E_x = 3.35$, measured Q . Magnetic spectrograph.

I. INTRODUCTION

The $T = 2$ states in the mass-12 nuclei have a number of unusual properties which have singled them out for detailed experimental and theoretical investigation in recent years. Three members of the lowest isobaric quintet are now definitely known, in ^{12}Be , ^{12}B , and ^{12}C (see Ref. 1) and preliminary evidence for ^{12}O has been obtained by Kekelis *et al.* via the $^{16}\text{O}(^4\text{He},^8\text{He})$ reaction.² However, the $T = 2$ state in ^{12}N has not been detected despite a number of efforts.¹ The cross section for the $^{14}\text{C}(p,t)^{12}\text{C}$ (27.6) reaction is significantly lower than the typical magnitude, $\sim 100 \mu\text{b sr}^{-1}$, for analogous reactions to $T = 2$ states in other 4n nuclei. Although this may be due in part to the extremely negative Q -value, -32 MeV, Barker³ has interpreted both the low cross section and discrepancies in the Coulomb energies in terms of configuration mixing. (A particularly interesting feature of Barker's calculations is the implication that there may be another low-lying 0^+ , $T = 2$ state, possibly the first excited $T = 2$ state.)

Many experimental efforts to observe the lowest $T = 2$ state in ^{12}C as an isospin-forbidden resonance have been made. Black, Caelli, and Watson⁴ investigated the $^9\text{Be}(^3\text{He},\gamma\gamma)$, $^{10}\text{B}(d,p)$, $^{10}\text{B}(d,\alpha)$, and $^{10}\text{B}(d,\gamma\gamma)$ reactions, observing a small anomaly only in $(^3\text{He},\gamma\gamma)$. Subsequent investigations,^{5,6} however, did not find that resonance at a level of sensitivity substantially greater than the original experiment. Snover,⁷ and more recently Nathan and Noé,⁸ have sought to observe the resonance in radiative proton capture, also without success. These results appear to indicate that the particle widths in all the accessible (ground-state) channels are very small. Ashery *et al.*⁹ investigated the particle decays of the $T = 2$ state and found a ground-state proton branch $\Gamma_p/\Gamma \leq 0.1$, which is presumably consistent with the estimate made by Nathan and Noé, $\Gamma_p/\Gamma < 0.006$. Very recently, the particle decays have been investigated at

Princeton University,¹⁰ and a preliminary analysis indicates that both the ground-state proton and ground-state deuteron decay branches are less than 5%. The ^3He decay could not be investigated. While it may well be that the ground-state particle widths are indeed all very small, one other possibility exists that would explain the non-observation of the state, and that is an error in the excitation energy. Four measurements of the energy have been made,^{9,11-13} all in reasonable agreement, giving a weighted average of 27.591 (12) MeV. The motivation for the present work was to check that result and to improve its precision with a view to future resonance searches.

II. EXPERIMENTAL METHOD

The $^{14}\text{C}(p,t)^{12}\text{C}$ (27.6) reaction is far from ideal as a basis for a mass measurement. The low cross section becomes even smaller at the forward angles preferred for kinematic reasons. (At 45 MeV and a laboratory angle of 22° , the cross section is found to be approximately $5 \mu\text{b sr}^{-1}$.) The Q value is so negative that there are no suitable (p,t) reactions that could serve as direct calibrations, and rather high beam energies are required. The thickness and uniformity of the targets (made by cracking ^{14}C -enriched acetylene onto a gold backing) are matters of concern when high precision is desired. There is also a continuous triton background, partly from $T <$ states in ^{12}C and partly from the backing, which exacerbates the cross section problem.

Nolen, Hamilton, Kashy, and Proctor¹⁴ have described a technique for precision mass measurements which makes use of nuclear emulsions in a magnetic spectrograph. The reaction products from the reaction under investigation are recorded simultaneously with suitably chosen calibration lines. Then, by a linearized least squares fit, all the unknown parameters in the experiment, the beam energy, the reaction angle, the spectrograph focal plane calibration and the target thickness, can be determined

Cohesion of nuclear matter

George Bertsch and David Munding

Department of Physics and Cyclotron Laboratory, Michigan State University, East Lansing, Michigan 48824

(Received 27 December 1977)

The fused system formed in a heavy-ion collision breaks up immediately if the longitudinal energy per particle is greater than 2 MeV/A (c.m.). This result is derived using the classical theory of compression and rarefaction waves. The dependence of the result on the equation of state of nuclear matter is slight. There is some dependence on the range of the interaction.

[NUCLEAR REACTIONS Heavy ion reactions, nuclear matter, fragmentation.]

To obtain a qualitative understanding of heavy-ion collisions at higher bombarding energies, it is desirable to delineate the conditions for the fused system of nuclear matter to break up immediately, and the conditions for the system to remain fused. On the experimental side, the phenomenon of deep inelastic scattering shows that rapid fission is extremely probable when the mass of the system is large enough, even when the bombarding energy is relatively low. On the theoretical side, numerical studies of one-dimensional dynamics^{1,3} show that nuclear matter is not very strong: when the energy exceeds 2 MeV/nucleon, the fused system quickly splits apart. At first sight this breakup threshold seems low, since the most obvious controlling parameter is the equilibrium binding energy which has a value of 16 MeV/A. In this note we will show how this result arises from continuum mechanics.

Before proceeding, it is necessary to justify the application of continuum mechanics and one-dimensional models. It is always possible to define for a many body system the local density $\rho(r)$, current $\vec{j}(r)$, and the stress tensor S_{ij} . The equation of continuity relating ρ and \vec{j} can be derived from the quantum equation of motion.⁴ An equation of motion for the $\partial\vec{j}/\partial t$ can also be derived, relating it to S_{ij} . Classically, a closed system of equations is obtained when S_{ij} is expressed in terms of local quantities such as ρ and the gradient \vec{j} . The simplest approximation, giving the Euler equation of hydrodynamics, is that S_{ij} depends on ρ alone:

$$S_{ij} = \delta_{ij} P(\rho).$$

In this situation the motions in the three dimensions are strongly coupled together. On the other hand, if the stress associated with a distortion $\epsilon_{ij} = \frac{1}{2}(\nabla_i u_j + \nabla_j u_i)$ is given by

$$S_{ij} = c \epsilon_{ij},$$

then the three directions are essentially uncoupled

in the equation of motion. In mean field theory, with parameters in a range considered reasonable for nuclear matter, there is in fact considerable decoupling. More compelling than the theoretical argument is the experimental evidence on the dynamics from the giant multipole vibrations. There is a well-established quadrupole mode at $63/A^{1/3}$ and recent evidence for a monopole at $80/A^{1/3}$ (Ref. 5). The near degeneracy of these two modes implies that distortional motion along the different coordinate axes is nearly uncoupled, and thus the motion is essentially one dimensional. Of course, we know that the fluid description also has a realm of validity. The liquid drop formula for nuclear binding describes the potential energy of the usual fission process quite well, at least before the scission point. The difference is the time scale. The stress tensor remains anisotropic on a time scale characteristic of the damping of the giant quadrupole state. The giant quadrupole has a width of about 3 MeV in ²⁰⁸Pb, which implies a damping time for the stress tensor of about 60 fm/c. The usual fission of nuclei near their ground state takes a much longer time. An appropriate measure is perhaps the residual interaction between quasiparticles. Estimating this as 100 keV, the isotropic fluid description holds for times ~ 2000 fm/c.

We will consider two basic models for the stress tensor. The first is the Thomas-Fermi model, in which the particles are assumed to occupy a Fermi sphere of minimum radius. In that case the stress is isotropic and given by

$$S_{ii} = P = \frac{\partial E}{\partial V} = \rho^2 \frac{\partial E/A}{\partial \rho}. \quad (1)$$

This requires knowledge of the relationship between energy and density. We will follow Zamick⁶ and parametrize the equations of state by an equation of the form

$T = 3/2$ levels in ^{15}F and ^{15}O

W. Benenson, E. Kashy, A. G. Ledebuhr, R. C. Pardo, R. G. H. Robertson, and L. W. Robinson
Cyclotron Laboratory and Physics Department, Michigan State University, East Lansing, Michigan 48824

(Received 28 November 1977)

The $^{20}\text{Ne}(^3\text{He}, ^8\text{Li})$ reaction has been used to study the particle-unstable nucleus ^{15}F . The ground state of ^{15}F is observed as a broad peak at a mass excess of 16.9 ± 0.2 MeV with a width greater than 900 keV. A well defined narrower peak is observed at a mass excess of 18.088 ± 0.025 MeV and with a width of 240 ± 30 keV. It is shown to be the mirror of the $5/2^+$ first excited state of ^{15}C . The analog of the $5/2^+$ state was observed in ^{15}O at $E_x = 12.255 \pm 0.013$ MeV. This state is shown to proton decay to the $T = 1$ first excited state of ^{14}N and to have a width of 135 ± 15 keV.

NUCLEAR REACTIONS $^{20}\text{Ne}(^3\text{He}, ^8\text{Li})^{15}\text{F}(p, t)^{15}\text{O}$ ($T=3/2$) measured reaction Q values, $\Gamma_{c.m.}$; deduced mass excesses, excitation energies. Deduced coefficients IMME.

I. INTRODUCTION

Because it would be the mirror of ^{15}C , which has a $1/2^+$ ground state, and because it is predicted to be approximately 2 MeV unbound to proton decay, one would expect ^{15}F to have a very broad ground state. The situation is in fact very similar to ^{11}N , the ground state of which would also be $1/2^+$ and has proven to be unobservable in multinucleon transfer reactions.¹ The first excited state of ^{11}N , however, was observed as a broad, asymmetric peak in the $^{14}\text{N}(^3\text{He}, ^6\text{He})$ reaction.¹ The present experiment is one of the first attempts to measure the mass and energy levels of ^{15}F . The reaction used was $^{20}\text{Ne}(^3\text{He}, ^8\text{Li})$ at 75 MeV, and the resulting spectra show clear evidence for the $5/2^+$ first excited state and somewhat weaker evidence for the ground state.

To support the above identifications of ^{15}F states, the $^{17}\text{O}(p, t)^{15}\text{O}$ reaction was used to search for the unknown analogs of the ^{15}F levels in ^{15}O . The first excited state analog was located and identified both by its spin and isospin. The resulting completed mass quartet agrees well with the isobaric multiplet mass equation.²

II. EXPERIMENTAL METHOD AND RESULTS

In the present paper three separate experiments will be discussed. The first is the study of ^{15}F by the $^{20}\text{Ne}(^3\text{He}, ^8\text{Li})$ reaction, and the other two are investigations of $T = 3/2$ states in ^{15}O . Details and results of these experiments are described below.

A. $^{20}\text{Ne}(^3\text{He}, ^8\text{Li})$ Reaction

Spectra from the $^{20}\text{Ne}(^3\text{He}, ^8\text{Li})$ reaction were taken at 9° , 10° , 11° , and 13° utilizing two different gas target systems. About $1 \mu\text{A}$ of 74.5 MeV ^3He particles from the Michigan State University Cyclotron bombarded the target, and the ^8Li -particles were detected on the focal plane of an Engle split-pole spectrograph using a method identical to that described previously.³ The 10° data were taken in the same fixed-angle gas cell which was used in other mass measurements.⁴ The 9° , 11° , and 13° data were taken in a new cell which has variable angle capability by means of the conventional extended exit foil and movable collimator. The exit foil thickness which was required, 2.2 mg/cm² of Ni, led to greater energy loss corrections than were made for the fixed cell, which used a 0.45 mg/cm² Mylar foil. Both cells held a gas pressure of 150 to 200 torr of isotopically enriched (99.95%) ^{20}Ne .

A previous run with a non-enriched Ne at 10° was not included in the present analysis since the 9.5% of ^{21}Ne and ^{22}Ne seem to produce a non-negligible background.

A sum of all the 10° data ($Q = 75\,000 \mu\text{C}$) is shown in Fig. 1. The peak labelled A is due mainly to the ground state of ^{15}F which is apparently very broad since it can decay with an $L = 0$ proton of an energy right at the top of the Coulomb barrier. Some of the yield may be attributable to the $^{20}\text{Ne}(^3\text{He}, ^8\text{Li})^{14}\text{O} + p$ reaction, but it is impossible to ascertain how much. In addition, the upper edge of peak A is obscured by the peak labelled B which is the mirror of the $5/2^+$, 740 keV state of ^{15}C as will be shown below. The cross section for producing this state at 10° is quite large, $0.25 \pm 0.02 \text{ u b/sr}$, as would be expected from simple shell model considerations. The data taken at 9° , 11° , and 13° have somewhat poorer statistics but show that the peak labelled B has the correct kinematics for the ^{15}F state. All the data were used in determining the mass excess and width of the peak as described below. The peak labelled C corresponds to both ^8Li and ^{15}F being left in their first excited states, and its shape shows the effect of the decay in flight of ^8Li . A small peak just to the left of C is the $^{14}\text{N}(^3\text{He}, ^8\text{Li})$ reaction from a slight air contamination of the gas.

The energy scale was calibrated by means of the

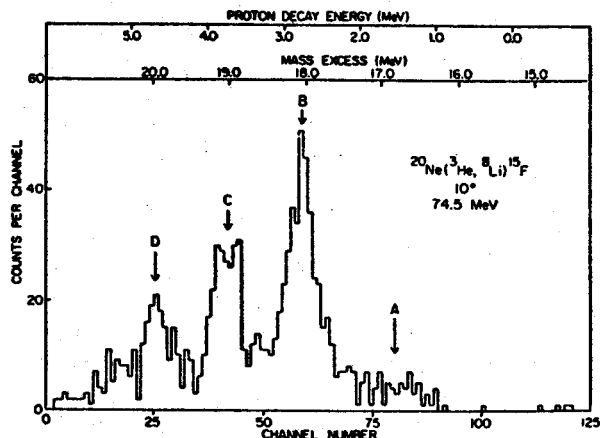


FIG. 1. Spectrum from the $^{20}\text{Ne}(^3\text{He}, ^8\text{Li})$ reaction at 10° and 74.5 MeV.

$^{31}\text{P}(^3\text{He}, d)^{32}\text{S}$ reaction at 25 MeV

J. Kalifa, J. Verotte, Y. Deschamps, F. Pougheon, G. Rotbard, and M. Vergnes
Institut de Physique Nucléaire, BP 1, 91406 Orsay, France

B. H. Wildenthal*

Institut de Physique Nucléaire, BP 1, 91406 Orsay, France
and Cyclotron Laboratory † Michigan State University, East Lansing, Michigan 48824

(Received 27 December 1977)

The $^{31}\text{P}(^3\text{He}, d)^{32}\text{S}$ reaction was investigated at 25 MeV incident energy. One-hundred and eleven levels up to an excitation energy of 12.5 MeV were observed using a split-pole magnetic spectrograph. The experimental angular distributions were analyzed with the distorted-wave Born approximation. The optical model parameters used in the distorted-wave Born-approximation calculations were obtained from a fit to elastic ^3He scattering data taken on ^{31}P at 25 MeV. Gamow functions were used as form factors for the transferred proton in the case of unbound states. Values of the transferred orbital angular momenta l and spectroscopic strengths were obtained for sixty levels, with many odd-parity levels being observed above 9 MeV excitation. Spin and parity assignments were made upon the basis of the l values obtained from the shapes of the angular distributions and upon comparison with the results of other reactions. Isospin assignments were made by comparison with ^{32}P levels. Except for the $l_p = 1, T = 0$ transfers, most of the observed spectroscopic strength is concentrated into a few levels. The existence of a T -mixed doublet of levels, $J^\pi = 1^-$, is suggested in the 11 MeV region of excitation. The excitation energies and spectroscopic strengths are compared with results of a recent shell-model calculation.

[NUCLEAR REACTIONS $^{31}\text{P}(^3\text{He}, d), ^{31}\text{P}(^3\text{He}, ^3\text{He}), E = 25$ MeV; measured $\sigma(E_d, \theta)$, ^{32}S deduced levels, l, J, π, T , spectroscopic strengths; measured $\sigma(\theta)$, deduced optical model parameters. DWBA analysis using Gamow functions as form factors.]

I. INTRODUCTION

The most extensive study of the nucleus ^{32}S through the $^{31}\text{P}(^3\text{He}, d)^{32}\text{S}$ reaction was done some years ago at 12 MeV by Graue *et al.*¹ In this study levels were observed up to 9.5 MeV. According to the sum rules of MacFarlane and French² most of the $l = 0$ and 2 stripping strengths were observed, but a large part of the $l = 1$ and 3 strengths was missing and is expected to lie at higher excitation energies. The first aim of the present work is to extend the knowledge of the $^{31}\text{P}(^3\text{He}, d)^{32}\text{S}$ reaction to levels above 9.5 MeV, and especially to look for the $l = 1$ and 3 strength which is carried by the few levels ($E_x = 10.0$ – 10.4 MeV, $J^\pi = 2^-, 3^-,$ and $4^-, T = 1$) strongly populated in the $^{31}\text{P}(p, \gamma)^{32}\text{S}$ reaction.³ Towards this aim levels in ^{32}S were observed up to an excitation energy of 12.5 MeV and the angular distributions obtained were analyzed with the distorted-wave Born approximation (DWBA). Special attention was given to proton-unbound levels above $E_x = 8864$ keV. It was possible to identify some of the currently observed stripping levels with resonance levels previously observed in proton or/and α -capture reactions. Isospin assignments to some ^{32}S levels were made by comparison with spectroscopic information

from the $^{31}\text{P}(d, p)^{32}\text{P}$ reaction.⁴

Using the comprehensive set of spectroscopic factors and energies obtained in the present work, augmented by the results of previous proton stripping^{1,5} studies and by results of recent pickup experiments,^{6,7} the second aim of the present study is to evaluate the present understanding of the nuclear structure of ^{32}S as it is specifically revealed in the single-nucleon stripping process. To this end, the experimental results are discussed in terms of sum rules and in comparison to a new shell-model calculation for the positive-parity levels of ^{32}S .

II. EXPERIMENTAL PROCEDURES

A 25 MeV ^3He beam from the Orsay MP tandem Van de Graaff accelerator was used for the present experiment. The targets (60 – $120 \mu\text{g}/\text{cm}^2$) were prepared by evaporation in vacuum of red phosphorus⁸ on carbon backings about $15 \mu\text{g}/\text{cm}^2$ thick. A surface barrier detector mounted inside the scattering chamber at $\theta_{\text{lab}} = 53^\circ$ with respect to the beam direction was used as a monitor during the angular distribution measurements.

Deuterons were momentum analyzed with an Enge split-pole magnetic spectrograph and were

Search for parity mixing in the $^{93}\text{Tc } 17/2^-$ isomer: measurements of internal conversion coefficients*

B. A. Brown, R. A. Warner, and L. E. Young

Cyclotron Laboratory, Michigan State University, East Lansing, Michigan 48824

F. M. Bernthal

Departments of Chemistry and Physics, and Cyclotron Laboratory, Michigan State University, East Lansing, Michigan 48824

(Received 11 August 1977)

The internal conversion coefficients were measured for several transitions in ^{93}Tc with an electron spectrometer and a Ge(Li) detector. The $^{92}\text{Mo}(\alpha, p2n)$ reaction was used to study the decay of the isomeric $\tau = 15 \mu\text{sec } 17/2^-$ level at 2185.3 keV as well as the decay of the prompt $17/2^+$ level at 2185.0 keV. Due to parity mixing the wave function for the $17/2^-$ isomeric level may have the form $|17/2^- \rangle + \alpha |17/2^+ \rangle$ where α is small. The experimental K -shell conversion coefficients for the $17/2^- \rightarrow 13/2^+$ and $17/2^+ \rightarrow 13/2^+$ transitions imply $\Gamma(E2, 17/2^- \rightarrow 13/2^+)/\Gamma(E2 + M2 + E3, 17/2^+ \rightarrow 13/2^+) \leq 0.33$. The energy difference between the prompt and delayed γ -ray transitions to the $13/2^+$ level was measured to be 0.32 ± 0.03 keV. These results imply $|\langle 17/2^+ | H_{pv} | 17/2^- \rangle| \leq 0.13$ eV for the matrix element of the parity violating Hamiltonian.

NUCLEAR REACTIONS $^{92}\text{Mo}(\alpha, p2n)$, $E = 43$ MeV measured pulse beam electronic timing, I_{ce} , I_γ , E_γ ; deduced α_K , γ multipolarity, parity mixing. Enriched target, electron spectrometer, Si(Li) and Ge(Li) detectors.

I. Introduction

In a previous study¹ of ^{93}Tc , an isomeric $17/2^-$ level, $\tau = 15 \mu\text{sec}$, at 2185 keV was found to lie only about 0.4 keV above a prompt $17/2^+$ level. The notation $17/2^-$ refers to the state with a possible mixed parity, $|17/2^- \rangle = |17/2^- \rangle + \alpha |17/2^+ \rangle$. The $17/2^+$ level decays to the $13/2^+$ level and shell-model calculations² give an estimate of $\tau \approx 30$ psec for its mean lifetime. Since the lifetimes of the $17/2^+$ and $17/2^-$ levels differ by a factor of 5×10^5 , the $17/2^- \rightarrow 13/2^+$ decay is extremely sensitive to a small mixing of the $17/2^+$ into the $17/2^-$ level which can originate from a parity-violating weak interaction component in the nuclear force². In Ref. 1 a limit of $|\langle 17/2^+ | H_{pv} | 17/2^- \rangle| \leq 0.34$ eV was obtained for the matrix element of the parity-violating Hamiltonian. The $17/2^-$ isomeric decay scheme is shown in Fig. 1.

Many experiments have shown evidence for parity violation in nuclear transitions². These experiments serve as a unique test for the predictions of various models of the weak interaction concerning the interaction of hadrons with hadrons. Of particular interest is the presence of neutral currents predicted by the Weinberg-Salam model³. Neutral current events in both leptonic and semileptonic processes have been observed but their presence in purely hadronic interactions is of fundamental importance to the theories. The purely hadronic neutral current interactions are expected to be most easily observed in the nucleon-nucleon interaction.

In order to unambiguously relate the parity violations observed in nuclear transitions to the strength of the parity-violating Hamiltonian operator, several conditions are necessary. First, it is important to have a reliable microscopic model of the states involved, and this condition is simplified if the effect is mostly due to the mixing of two nearly degenerate levels. A good example of this is the $J = 1/2$ doublet in ^{19}F which has been studied by Adelberger et al.⁴ Here the $1/2^-$ state and $1/2^+$ ground state are separated by 110 keV and the next $J = 1/2$ levels

are several MeV higher; the energies of these states are well described in the shell model with $p_{1/2} d_{5/2} s_{1/2}$ configurations. ^{93}Tc is very similar in this regard. The $J = 17/2$ levels are separated by only about 0.4 keV and the energies are well described by the shell model with predominant configurations of $g_{9/2} p_{1/2}$ and $g_{9/2} p_{1/2}^2$ for $17/2^-$ and $17/2^+$, respectively.

In addition, the parity violating matrix element should be large and not dominated by cancellation effects due to nuclear structure. The parity violating Hamiltonian operator is expected to have a strength on the order of 1 eV.² The matrix element

$$|\langle ^{19}\text{F } 1/2^+ | H_{pv} | ^{19}\text{F } 1/2^- \rangle| = 1.2 \pm 0.6 \text{ eV}$$

obtained from the ^{19}F γ -ray asymmetry experiments⁴ is thus considered large. In contrast, the very small value of

$$|\langle ^{180}\text{Hf } 8^+ | H_{pv} | ^{180}\text{Hf } 8^- \rangle| =$$

$$(1.2 \pm 0.2) \times 10^{-6} \text{ eV}$$

implied from the ^{180}Hf measurements⁵ is an example of the large cancellation effects which can occur, in this case due to the $\Delta K = 8$ change in the intrinsic rotational wave functions.

In Sec. IV these disparate values for the matrix elements from ^{19}F and ^{180}Hf are shown to be closely scaled to the experimental electric dipole matrix elements between the same states. Using a typical E1 strength for the mass-90 region, this empirical scaling relation implies a parity violating matrix element on the order of 1.0 to 0.1 eV for ^{93}Tc . The H_{pv} matrix element may be reduced in ^{93}Tc compared to ^{19}F because the $17/2^-$ differs from the $17/2^+$ configuration by a $\Delta j = 4$ or 5 change in one orbital.

The scaling relation implies an H_{pv} matrix element in ^{93}Tc comparable to the upper limit of 0.34 eV. This implies that the E2 component in the $17/2^- \rightarrow 13/2^+$ transition may be quite large. In this work we report on a

$^{21}\text{Ne}(^3\text{He}, p)^{23}\text{Na}$ reaction

H. T. Fortune,* J. R. Powers,† and R. Middleton

Physics Department, University of Pennsylvania, Philadelphia, Pennsylvania 19104

H. Nann‡ and B. H. Wildenthal

Cyclotron Laboratory, Michigan State University, East Lansing, Michigan 48823

(Received 24 March 1978)

The reaction $^{21}\text{Ne}(^3\text{He}, p)^{23}\text{Na}$ has been investigated at a bombarding energy of 18.0 MeV, using enriched ^{21}Ne gas contained in a rotating gas cell. Angular distributions for the positive-parity states have been analyzed with the distorted-wave Born approximation, using transfer amplitudes from an $(sd)^7$ shell-model calculation. Agreement with experiment is good. Tentative correspondences are suggested for all experimental and theoretical levels below 6 MeV excitation. Low-lying negative-parity states are very weakly populated.

NUCLEAR REACTIONS $^{21}\text{Ne}(^3\text{He}, p)$, $E = 18.0$ MeV; measured $\sigma(E_p, \theta)$. ^{23}Na deduced levels L, J, π . DWBA analysis with shell-model wave functions. Enriched gas target.

I. INTRODUCTION

The most severe critique of existing nuclear shell-model theory is its ability to predict correctly observables for nuclei in the middle of a shell.

A rather sensitive test of the wave functions of the initial and final states can be provided by the comparison of experimental two-nucleon transfer differential cross sections with microscopic distorted-wave Born approximation (DWBA) calculations based on matrix elements of the coupled two-particle creation (or annihilation) operator.

In the case of the reaction under study here $^{21}\text{Ne}(^3\text{He}, p)^{23}\text{Na}$, most of the levels in the final nucleus ^{23}Na below 6 MeV of excitation have known spin and parity. All of them that are known to have even parity can be identified with states predicted in an $(sd)^7$ shell-model calculation.² Except for a $K^\pi = \frac{7}{2}^+$ rotational band that is predicted, but not observed, the agreement between calculated and measured energies is very good, as depicted in Fig. 1.

Spectroscopic amplitudes calculated from the wave functions of Ref. 2 were used with DWBA calculations to predict the shapes and relative differential cross sections of transitions to even parity states in ^{23}Na . The ability to reproduce the shape of the experimental angular distributions and the consistency of the ratio of the measured and calculated cross sections then give a measure of the goodness of the theoretical wave functions.

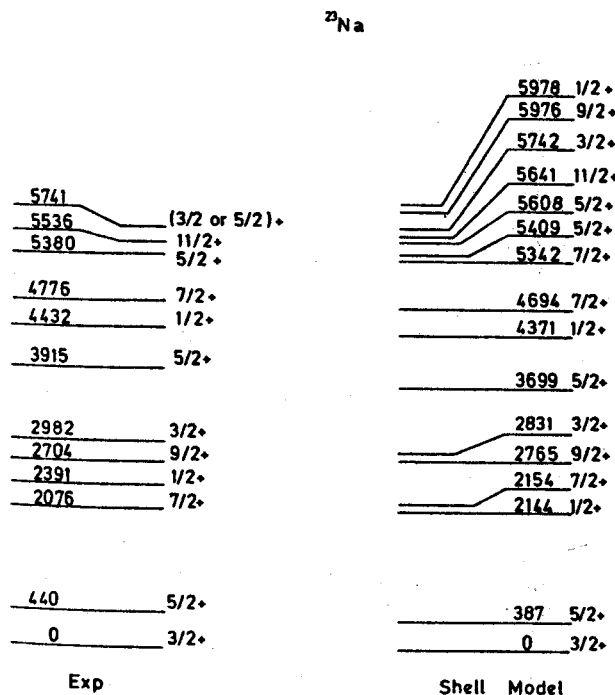


FIG. 1. Experimental levels of ^{23}Na (left, Ref. 1) known to have positive parity prior to present work compared with energies calculated in an $(sd)^7$ basis (right, Ref. 2). Only levels below 6 MeV are included.

II. EXPERIMENTAL PROCEDURE AND RESULTS

The experiment was performed with an 18-MeV ^3He beam from the University of Pennsylvania tan-

Threshold pion absorption in nuclei*

G. F. Bertsch and D. O. Riska

Department of Physics and Cyclotron Laboratory, Michigan State University, East Lansing, Michigan 48824

(Received 25 January 1978; revised manuscript received 10 April 1978)

We attempt to explain threshold pion absorption in nuclei using simple pion rescattering mechanisms. While the model is successful in the case of the deuteron it leads to 10–30% too small absorption rates in other nuclei. We also study a $\rho\omega$ exchange absorption mechanism that does not act in the deuteron, but find that it can only remove a small part of the remaining discrepancy. The two-nucleon absorption mechanism accounts for 75% of the imaginary part of the S -wave pion nucleus optical potential.

[NUCLEAR REACTIONS Pion absorption calculated at threshold in light nuclei
 ^2H , ^4He , ^{12}C , ^{16}O , ^{20}Ne , and nuclear matter.]

I. INTRODUCTION

Pion absorption in nuclei has been discussed extensively in recent literature.¹ The lack of success in early attempts to explain threshold pion absorption with single nucleon mechanisms has led to a general consensus that the absorption mechanism involves at least two nucleons. Even so it was not long ago still claimed that "by and large, pion absorption in nuclei is still a mystery."² The recent progress in calculations of pion absorption in the deuteron using simple two-body rescattering mechanisms^{3–5} suggests that it is now high time to reduce some of the "mystery" surrounding pion absorption in nuclei.

In this paper we attempt to explain pion absorption at threshold with the assumption that the dominant mechanism is absorption of a virtual pion, created in a scattering of the initial physical pion. To describe the rescattering vertex we use the phenomenological zero range $\pi\pi NN$ interaction Hamiltonian employed by Woodruff⁶ and later by Koltun and Reitan.⁷ This interaction involves two coupling parameters which are determined by the pion nucleon S -wave scattering lengths.

With this model we obtain perfect agreement with the empirical absorption rate for the deuteron, but find that the calculated absorption rates in other nuclei are 10–30% too small. These results represent an improvement over the earlier situation where the predicted absorption rate in ^4He was found to be too large by about 50% (Refs. 8 and 9) and in nuclear matter too small by a factor 3.¹⁰ To understand the remaining discrepancy in nuclei other than the deuteron we also consider a two-body process involving exchange of a ρ and a ω meson which does not act in the deuteron. We find, however, that this process can increase the calculated absorption rate by at most 5% and that

it is thus insufficient to remove all of the discrepancy.

It was recently suggested that the off-shell pion-nucleon scattering amplitude should differ considerably from the on-shell one.¹¹ The smooth off-shell behavior of the pion rescattering amplitude we employ and the subsequent fair (perfect in the deuteron case) agreement with the empirical absorption rates in general indicates that no drastic off-shell extrapolation of the amplitudes is required.

The present paper falls into six sections. In Sec. II we explain the pion rescattering model and the method of calculating the imaginary parts of the S -wave scattering lengths. In Sec. III we give the numerical results for pion rescattering in light nuclei and study the effect of wave function correlations. In Sec. IV we calculate the imaginary part of the S -wave pion-nucleus optical potential using the Fermi gas model. In Sec. V we develop the absorption operator involving pion absorption into a ρ and an ω meson and calculate its magnitude. Finally, we give a concluding discussion in Sec. VI.

II. ABSORPTION RATE FOR PION RESCATTERING

A. General expressions for the absorption rate

The rate for pion absorption in a nucleus is

$$\Gamma = 2\pi \sum_{if} \delta(E_f - E_i - \omega) |T_{if}|^2, \quad (2.1)$$

where T_{if} is the matrix element of the absorption operator and the sum runs over all final states. The energies of the nuclear ground state and final

INTERACTIONS FOR INELASTIC SCATTERING DERIVED FROM REALISTIC POTENTIALS †

G. BERTSCH, J. BORYSOWICZ and H. McMANUS

*Cyclotron Laboratory and Department of Physics, Michigan State University, East Lansing,
 Michigan 48824*

and

W. G. LOVE

*Cyclotron Laboratory and Department of Physics, Michigan State University, East Lansing,
 Michigan 48824*

and

Department of Physics and Astronomy ††, The University of Georgia, Athens, Georgia 30602

Received 30 June 1976

(Received 21 February 1977)

Abstract: An effective local interaction for inelastic scattering is derived by fitting the matrix elements of a sum of Yukawas and, for the tensor force, other closely related forms, to three selected sets of G -matrix elements. The ranges were selected to ensure OPEP tails in the relevant channels as well as a short-range part which simulates the “ σ -exchange” process. Some of the implications of the various parts of the interaction are discussed in a distorted-wave context.

1. Introduction

This report describes a set of interactions for inelastic scattering which are derived from the nucleon-nucleon potentials of Hamada and Johnston ¹⁾ and Reid ²⁾ and from the oscillator matrix elements of Elliott ³⁾. The interactions are devised to be used with nuclear scattering codes. Exchange terms must be included. We are not discussing in this paper pseudopotentials which include approximately the effects of exchange. The route from the nucleon-nucleon potential to an inelastic scattering interaction is long and tedious, hence the necessity of a thorough description. The resulting potentials do not necessarily provide a good fit to experimental inelastic scattering data, but we hope that they will provide a fairly unambiguous prediction of inelastic scattering from the fundamental nucleon-nucleon interaction. In current distorted-wave programs ^{4, 5)}, the effective nucleon-nucleon interactions in inelastic scattering are frequently taken to be of the convenient forms †††

$$\begin{aligned}
 V &= \sum_i V_i Y(r_{12}/R_i), \quad \text{central,} \\
 V &= \sum_i V_i Y(r_{12}/R_i) L \cdot S, \quad \text{spin-orbit,}
 \end{aligned}
 \tag{1}$$

† Research sponsored in part by the National Science Foundation.

†† Permanent address.

††† Eq. (2) is from ref. ⁴⁾, and eq. (3) from ref. ⁵⁾.

THE $^{40}\text{Ca}(\alpha, d)^{42}\text{Sc}$ REACTION †

H. NANN, W. S. CHIEN, A. SAHA and B. H. WILDENTHAL

Cyclotron Laboratory and Department of Physics, Michigan State University, East Lansing, Michigan 48824

Received 1 June 1977

Abstract: Angular distributions of the $^{40}\text{Ca}(\alpha, d)^{42}\text{Sc}$ reaction at $E_\alpha = 40$ MeV have been measured for states in ^{42}Sc up to an excitation energy of 5.2 MeV. Assignments of the L -transfer are made on the basis of the characteristic shapes of the angular distributions. A strong $L = 6$ transition to a state at 3.61 MeV in the ^{42}Sc is observed. Evidence for the fragmentation of the $(f_{7/2})^2_{5,0}$ and $(f_{7/2}p_{3/2})_{5,0}$ configurations into the 5^+ states at 1.51 and 3.09 MeV is discussed.

E NUCLEAR REACTION $^{40}\text{Ca}(\alpha, d), E = 40$ MeV: measured $\sigma(E_d, \theta)$, ^{42}Sc deduced levels, L -transfer. Enriched target.

1. Introduction

The low-lying states of ^{42}Sc can be described in the terms of the simple shell model as a proton and a neutron in the $f_{7/2}$ orbital outside the doubly closed ^{40}Ca core. These states are important in providing the $(f_{7/2})^2$ matrix elements of the residual two-body nuclear interaction for shell-model calculations^{1–3}. However, the relation of the experimental situation to the simple $(f_{7/2})^2$ model is not so simple, since there exist low-lying states which originate from core-deformed configurations mixed with the two-particle shell-model states⁴. Even without these core-deformed configurations, admixtures of the $(f_{7/2}p_{3/2})$ configurations into the $(f_{7/2})^2$ configurations complicate the extraction of reliable $(f_{7/2})^2$ two-body matrix elements.

Two-nucleon transfer reactions such as $(^3\text{He}, p)$ or (α, d) are well suited to investigate the two-particle nature of the low-lying states of ^{42}Sc . Angular distributions of the $^{40}\text{Ca}(^3\text{He}, p)^{42}\text{Sc}$ reaction have been analyzed in the past with DWBA calculations based on shell-model wave functions by Barz *et al.*⁵) and Pühlhofer⁶). These wave functions describe the ^{42}Sc states alternatively with and without excited-core configurations. Fair agreement between the calculated and experimental differential cross sections was obtained in these studies.

The $^{40}\text{Ca}(\alpha, d)^{42}\text{Sc}$ reaction has been studied to a lesser extent. Rivet *et al.*⁷) observed several strong deuteron groups leading to low-lying, high spin, $T = 0$ states in ^{42}Sc . Recently, Thomas and Skouras⁸) measured $^{40}\text{Ca}(\alpha, d)$ angular distributions for transitions to the first few states in ^{42}Sc and compared them to DWBA predictions

† Work supported by the National Science Foundation.

FOUR-PARTICLE ONE-HOLE STATES IN ^{43}Ca STRONGLY POPULATED BY THE $^{41}\text{K}(\alpha, d)$ REACTION[†]

H. NANN, W. S. CHIEN and A. SAHA

Cyclotron Laboratory and Department of Physics, Michigan State University, East Lansing, MI 48824

Received 28 December 1976

Abstract: Angular distributions of the $^{41}\text{K}(\alpha, d)^{43}\text{Ca}$ reaction have been measured at 40 MeV bombarding energy. Four-particle one-hole states in which the stripped proton-neutron pair occupies a $(f_{7/2})^2_{T=0}$ configuration coupled to the unperturbed ^{41}K core were identified by their characteristic $L = 6$ angular distributions. These states lie at 2.95, 3.37, 3.94, 4.13, 4.19, 4.59 and 4.89 MeV. Evidence for their $[(f_{7/2})^2_{T=0} d_{3/2}]$ 4p-1h character is discussed. Several other strong transitions were observed which show mixtures of $L = 4$ and $L = 6$ angular distributions.

E NUCLEAR REACTIONS $^{41}\text{K}(\alpha, d)$, $E = 40$ MeV, measured $\sigma(E_n, \theta)$, ^{43}Ca levels deduced L -transfer, J, π . Enriched target.

1. Introduction

Previous (α, d) studies¹⁻³⁾ have shown that stretched configuration high-spin states are preferentially excited because of the geometrical coefficients in the structure factor⁴⁾ and momentum mismatch conditions between the entrance and exit channels. This feature has been used in the present $^{41}\text{K}(\alpha, d)$ reaction to locate high-spin states in ^{43}Ca of 4p-1h character in which a transferred proton-neutron pair in the $(f_{7/2})^2_{T=0}$ configuration is coupled to the unperturbed 2p-1h configuration of the ^{41}K core. The transitions to these states are characterized by an orbital angular momentum transfer of $L = 6$.

High-spin levels in ^{43}Ca have been studied by Poletti *et al.*⁵⁾ via γ -ray spectroscopy of heavy-ion fusion-evaporation reactions, and decay schemes of the yrast levels together with suggested spin assignments were reported. De Voigt *et al.*⁶⁾ measured angular distributions of the $^{43}\text{Ca}(\alpha, \alpha')$ reaction and identified states resulting from coupling of an $f_{7/2}$ neutron to the 3^- and 5^- states in ^{42}Ca . These experiments have populated some of the 4p-1h states searched for in the present investigation of the $^{41}\text{K}(\alpha, d)^{43}\text{Ca}$ reaction. The juxtaposition of the three very different kinds of data should serve to illuminate the structural details of these states and, of course, to better fix their identities.

[†] Work supported in part by the US National Science Foundation.

FINE STRUCTURE IN THE GIANT RESONANCE REGION AND THE COLLECTIVE DIPOLE SPIN-FLIP EXCITATION IN ^{208}Pb

H. P. MORSCH[†], P. DECOWSKI^{**} and W. BENENSON

Cyclotron Laboratory, Michigan State University, East Lansing, MI 48824

Received 15 August 1977

(Revised 28 November 1977)

Abstract: Inelastic scattering of 40 and 45 MeV protons has been used to study the excitation region of 6–12 MeV in ^{208}Pb . This region is found to be strongly structured with states of different multipolarity. Fine structure peaks between 8.5 and 10 MeV show mainly quadrupole and octupole structure. The “giant” M1 excitations observed recently are strongly excited and are described by microscopic form factors. Several strongly excited states between 6 and 8.5 MeV show angular distributions of characteristic dipole ($L = 1$) structure. Ground-state widths derived from our inelastic cross sections are many times larger than measured in γ -induced reactions, and this indicates a structure different from isovector dipole. These states may represent a collective dipole spin-flip excitation ($L = 1, S = 1$) which in a simple collective picture can be interpreted as a collective dipole oscillation of spin-up particles against spin-down particles. Two of these states, at 7.40 and 7.92 MeV, were identified in 180° electron scattering as 2^- states. Derived $B(M2)$ values from our data are in excellent agreement with the electron scattering results. The other two states at 6.26 and 8.37 MeV may represent collective 1^- spin-flip excitations.

NUCLEAR REACTIONS $^{208}\text{Pb}(p, p')$, $E = 40, 45$ MeV; $^{208}\text{Pb}(\alpha, \alpha')$, $E = 48$ MeV; measured $\sigma(\theta)$. ^{208}Pb deduced strengths for $J = 1, 2, 3$ transitions in the region 6–12 MeV excitation, $B(M2)$.

1. Introduction

In the study of nuclear excitations strong collective motion is of particular interest. Apart from the well-known giant dipole resonance ($L = 1, T = 1$) and the more recently observed giant quadrupole resonance, there are several other possible collective excitations which have not been established experimentally, e.g. the giant monopole resonance. There are also other types of dipole excitations, e.g. magnetic dipole (1^+) and dipole spin-flip, which are of considerable interest. Magnetic dipole excitations have been subject of extensive studies for ^{208}Pb where, except for $2\hbar\omega$ excitations, only the h_{μ} proton and the i_{μ} neutron spin-flip is possible. Two M1 excitations have been established recently^{1,2} which yield a large portion of the M1 strength. In order to study collective modes in ^{208}Pb , we have measured inelastic

[†] Present address: Institut für Kernphysik, Kernforschungsanlage Jülich, Germany.

^{**} Present address: Institute of Experimental Physics, University of Warsaw, Warsaw, Poland.

STUDY OF THE $^{17}\text{O}(\alpha, d)^{19}\text{F}$ REACTION †

H. T. FORTUNE †† and L. R. MEDSKER †††

Physics Department, University of Pennsylvania, Philadelphia, Pennsylvania 19104, USA

and

H. NANN ‡ and B. H. WILDENTHAL

Cyclotron Laboratory, Michigan State University, East Lansing, Michigan 48823, USA

Received 12 October 1977

(Revised 8 February 1978)

Abstract: At a bombarding energy of 47.5 MeV, the $^{17}\text{O}(\alpha, d)^{19}\text{F}$ reaction is found to populate strongly only those positive-parity states that are known to consist predominantly of $(sd)^3$ configurations. Distorted-wave calculations based on transfer amplitudes computed from shell-model wave functions provide good agreement to the measured angular distributions – in both shape and magnitude.

E NUCLEAR REACTIONS $^{17}\text{O}(\alpha, d)$, $E = 47.5$ MeV; measured $\sigma(E_0, \theta)$. DWBA analysis. Enriched target.

1. Introduction

We have used the $^{17}\text{O}(\alpha, d)^{19}\text{F}$ reaction to investigate the low-lying states ¹⁾ of ^{19}F . At the high bombarding energy of 47.5 MeV employed here, the mechanism is undoubtedly one of direct two-nucleon transfer. The $\frac{3}{2}^+$ spin and parity of the $^{17}\text{O}(\text{g.s.})$ allows one to populate $(sd)^3$ states in ^{19}F with J^π values up to $\frac{13}{2}^+$ – the maximum J in an $(sd)^3$ $T = \frac{1}{2}$ spectrum. In fact, the kinematic preference for high- L transfer favors the high-spin final states. This fact was exploited in an earlier investigation ²⁾ of the $\frac{11}{2}^+$ states with the same reaction.

The aim of the present work was to compare the results of the highly selective $^{17}\text{O}(\alpha, d)$ reaction with those expected from a DWBA calculation that used as input a set of detailed wave functions ³⁾ that give a good account of the other properties of ^{19}F .

† Work supported by the National Science Foundation.

†† Presently at Oxford University on leave from the University of Pennsylvania.

††† Present address: Physics Department, Florida State University, Tallahassee, Florida 32306.

‡ Present address: LAMPF, Los Alamos, New Mexico 87544.

1.E.1:
2.G

Nuclear Physics A302 (1978) 186–204; © North-Holland Publishing Co., Amsterdam
Not to be reproduced by photoprint or microfilm without written permission from the publisher

LEVELS OF ^{52}Fe STUDIED WITH THE (p, t) REACTION †

P. DECOWSKI **, W. BENENSON, B. A. BROWN and H. NANN

Cyclotron Laboratory and Physics Department, Michigan State University, East Lansing, Michigan 48824

Received 28 December 1976

(Revised 2 March 1978)

Abstract: The $^{54}\text{Fe}(p, t)^{52}\text{Fe}$ reaction at 45 MeV has been used to study states of ^{52}Fe . Characteristic L -transfers in the angular distributions were used to assign ≈ 40 spins and parities. An $f_{7/2}$ shell model, with admixtures calculated in first-order perturbation theory, successfully accounts for both the location and strength of many of the observed levels.

E NUCLEAR REACTIONS $^{54}\text{Fe}(p, t)$, $E = 45$ MeV: measured $\sigma(E, \theta)$. ^{52}Fe deduced levels, L, J, π . Enriched target, magnetic spectrograph. Shell model calculation.

1. Introduction

Studies of the ^{52}Fe nucleus are important for understanding nuclear structure in the upper part of the $f_{7/2}$ shell. The structure of this nucleus has been investigated in the past with the ($^3\text{He}, n$) [refs. 1, 2] and (p, t) reactions ³⁻⁶. Spins and parities were assigned only to the most strongly excited states, which are characterized mainly by $L = 0, 2$ and 4 angular momentum transfers. Many of the weaker states remained unassigned, and there existed several controversies concerning even the stronger states.

The present high resolution experiment permits the finding of spins and parities for about forty levels with excitation energies up to 10 MeV. The comparison of the measured cross sections with the DWBA calculations provide some information about the distribution of $f_{7/2}^{-2}$ strength among the states. Admixtures of other orbitals which would drastically affect the cross section especially for $L = 0$ are accounted for by a first-order perturbation theory calculation.

2. Experiment

A beam of protons accelerated to an energy of 45 MeV by the Michigan State University Cyclotron bombarded a $250 \mu\text{g}/\text{cm}^2$ target of ^{54}Fe enriched to 96.7% which was deposited on $20 \mu\text{g}/\text{cm}^2$ ^{12}C foil. The position of triton groups on the

† Work supported in part by the National Science Foundation.

** On leave from the Institute of Experimental Physics of the University of Warsaw.

CRYOGENIC HELIUM JET AND RECOIL TIME-OF-FLIGHT APPARATUS*

R. G. H. ROBERTSON†

Department of Physics, Princeton University, Princeton, New Jersey 08540, U.S.A. and Cyclotron Laboratory, Michigan State University, East Lansing, Michigan 48824, U.S.A. +

T. J. BOWLES§ and S. J. FREEDMAN**

Department of Physics, Princeton University, Princeton, New Jersey, 08540, U.S.A.

Received 31 May 1977

An apparatus is described in which cyclotron-produced radioactivities are transported from the target area to a detection area in a stream of helium cooled to 92 K. The apparatus is intended for investigations of β -delayed particle-emitting nuclei and includes a time-of-flight path which allows mass identification of the nucleus responsible for each particle group. A theoretical model for the transport of atoms in pure gases is presented which explains quantitatively many aspects of existing data both at room temperature and at low temperatures.

1. Introduction

The helium-jet technique¹⁾ for rapidly transporting radioactive atoms from their point of production to another point has been much refined and improved since its inception. Until recently, it was thought that the addition to the helium of impurities, such as organic vapors or aerosol dispersions of micrometer-sized particles, was essential to high transport efficiency, and indeed efficiencies near unity have been reported²⁾. However, in some applications the presence of macroscopic amounts of non-volatile material in the gas stream is an undesirable or intolerable disadvantage. Such applications include the interfacing of the helium jet to certain types of ion source for mass spectrometry, precise studies of β -spectra, high-resolution measurements of delayed heavy-particle emission, and fundamental weak interaction studies which utilize the detailed spectral shapes of β -delayed particle lines. The particular application to which the present work is addressed is the extension of the limits of known radioactive nuclei to more proton-rich species, such as the $T_z = -2$ nuclei ^{20}Mg , ^{24}Si , ^{28}S , etc. That series of nuclei is expected to be characterized by β -delayed proton emission, which may permit location of the $T=2$ state in the

daughter nuclei, and a test of the isobaric multiplet mass equation to unprecedented precision. In addition, the β -delayed proton emission affords a means of measuring the mass number of the precursor, a vital step in the identification of a new nuclide in the presence of other, much more abundant nuclides. As will be explained below, exploitation of this scheme depends on continuous preparation of an extremely thin source.

Helium jet systems have been operated successfully with "pure" helium, particularly over short transport distances, but have generally been characterized by very low efficiencies and non-reproducible behavior. In addition, even with "pure" helium, sufficient impurities are usually present that the problems associated with impurity-loaded systems remain. Recently, however, a group at the University of Jyväskylä have conducted systematic studies of helium jets operated with very pure helium and, still more significantly, have discovered that dramatic increases in efficiency are possible if the entire source volume is cooled to the temperature of liquid air³⁻⁵⁾.

In the present paper a complete system associated with the Princeton University Cyclotron is described, in which a cryogenic (liquid-nitrogen cooled) helium jet is coupled to a recoil time-of-flight mass analyzer. Observations of some factors affecting transport efficiency are reported.

2. Helium jet system

2.1. THEORY OF OPERATION

In 1973 Äystö and Valli published³⁾ a very detailed series of observations on the absolute effi-

* Research supported by the U.S. National Science Foundation.

† Alfred P. Sloan Foundation Fellow.

+ Present address.

§ Present address: Physics Division, Argonne National Lab., Argonne, Illinois, U.S.A.

** Present address: Dept. of Physics, Stanford University, Stanford, California, U.S.A.

**ACTIVATION AND ANGULAR DISTRIBUTION MEASUREMENTS
OF ${}^7\text{Li}(p, n){}^7\text{Be}(0.0+0.429 \text{ MeV})$ FOR $E_p = 25\text{--}45 \text{ MeV}$:
A TECHNIQUE FOR ABSOLUTE NEUTRON YIELD DETERMINATION***

S. D. SCHERY

Cyclotron Laboratory, Michigan State University, E. Lansing, Michigan 48824, U.S.A.

and

Moody College, Texas A & M University, Galveston, Texas 77553, U.S.A.

L. E. YOUNG, R. R. DÖERING, SAM M. AUSTIN and R. K. BHOWMIK

Cyclotron Laboratory, Michigan State University, E. Lansing, Michigan 48824, U.S.A.

Received 19 April 1977 and in revised form 22 June 1977

Angular distributions of the combined ${}^7\text{Li}(p, n){}^7\text{Be}$ reactions to the ground and first excited state of beryllium have been measured at proton energies of 24.8, 35.0 and 45.0 MeV with a typical accuracy of 5%. The total cross section was also obtained at eleven energies between 24 and 45 MeV by activation techniques. The reaction is a potentially convenient source for neutrons, and absolute neutron fluence can be determined independent of beam current and target thickness measurement if the amount of ${}^7\text{Be}$ ($\tau_{1/2} = 53.4\text{d}$) produced in the reaction is measured. Following the proton irradiation the amount of ${}^7\text{Be}$ produced is determined by observation of the 0.478 MeV gamma rays from a 10.4% branch of ${}^7\text{Be}$ and this information is combined with the total cross sections and angular distributions to give the neutron fluence at the time of irradiation.

1. Introduction

The (p, n) reaction on ${}^7\text{Li}$ to the ground and first excited state of beryllium, ${}^7\text{Li}(p, n){}^7\text{Be}(0.0+0.429 \text{ MeV})$, provides a potentially convenient source of 20–50 MeV neutrons for neutron scattering experiments and for efficiency calibration of neutron detectors. The cross sections are large and the emitted neutrons are well separated from lower-energy neutrons. Lithium is a ductile metal that is moderately convenient to handle as a target material. The ${}^7\text{Li}$ nucleus is light and there is a substantial kinematic shift with angle. This feature provides a range of neutron energies for a single proton energy and can be useful for neutron detector calibration.

Precise measurements of the ${}^7\text{Li}(p, n){}^7\text{Be}(0.0+0.429 \text{ MeV})$ reaction are available up to 26 MeV^{1,2} but at higher energies measurements are more limited^{3,4} in both completeness and accuracy. We report measurements of the combined reactions, ground-state plus first-excited-state (0.429 MeV), in the proton energy range 25–45 MeV. Total cross sections for the combined reactions were obtained by an activation technique and were used for absolute normalization of angu-

lar distributions taken at 25, 35, and 45 MeV using neutron time-of-flight techniques.

The activation method takes advantage of the fact that the ground and 0.429 MeV states of ${}^7\text{Be}$ are the only particle-emission-stable states of ${}^7\text{Be}$, so that the activation cross section for the production of ${}^7\text{Be}$ is due exclusively to reactions leading to these states. The 53.4 d half-life of ${}^7\text{Be}$ is long enough that targets can be counted at a convenient time after activation. The production cross section can be measured by observing the 0.478 MeV gamma emission in ${}^7\text{Li}$ that follows the decay of ${}^7\text{Be}$ with a branching ratio of $10.4\% \pm 0.1\%$.

The availability of these cross sections permits simple measurements of the absolute neutron fluence from these reactions with better than 5% accuracy. No measurements of beam currents or target thickness are required if gamma decay measurements of ${}^7\text{Be}$ are made.

2. Experimental method

Angular distributions were obtained with the new beam swinger neutron time-of-flight facility at the Michigan State University Cyclotron Laboratory⁵). This system uses rotating magnets to change the angle of the incident beam while the

* Work supported in part by the U.S. National Science Foundation.

LETTERS TO THE EDITOR

A SIMPLE ION SOURCE FOR TARGET PREPARATION VIA ION BEAM SPUTTERING⁺

J. A. NOLEN JR., M. S. CURTIN and T. E. DYSON

Cyclotron Laboratory and Department of Physics, Michigan State University, East Lansing, MI 48824, U.S.A.

Received 1 December 1977

A simple glow discharge ion source has been developed and used to prepare thin-film nuclear targets of W, Pt, Mo, Zn, Ti and Si via ion beam sputtering with good efficiency for separated isotopes.

The utility of the ion beam sputtering method for the preparation of thin-film targets for nuclear physics has been discussed by Sletten and Knudsen¹⁾. They have used a duo-plasmatron ion source to generate an Ar⁺ beam with an energy of about 10 keV and an intensity of about 1 mA to prepare numerous isotopic targets, primarily of refractory materials such as W and Hf. Further development of the sputtering technique for target making has been done by Scarfe, Hanley and Purser²⁾, and by Wirth and Baumann³⁾ who utilize duo-plasmatron and Penning ion sources, respectively. The present communication describes a highly simplified ion source which has also proved very useful in the preparation of a wide variety of targets. Emphasis has also been placed on the use of a very efficient sputtering geometry and the application of the sputtering method to higher vapor pressure elements as well as the refractories.

An assembly drawing indicating the components of the simple glow discharge ion source is given in fig. 1. This is a modified version of the source manufactured by Edwards High Vacuum⁴⁾ and intended primarily for surface cleaning rather than target making. Modification of the Edwards system was necessary to achieve stable operation for long times (many hours) at power levels higher than originally intended for their source. An argon glow discharge is established in the confined region between the anode and cathode by applying a positive potential of 10–15 kV to the anode. The argon gas flow is adjusted via a needle valve to give a discharge current of about 1 mA between the anode and cathode. An Ar⁺ beam of about 100 μa emerges from the aperture in the cathode. The beam has a large energy spread with an average energy corresponding to about half of the voltage applied to the glow discharge. The divergence of the beam from the aperture is relatively small so that a spot size about 3 mm in diameter is obtained at a distance of 5 cm from the ion gun.

The present system differs from the original Ed-

⁺ Research supported in part by the U. S. National Science Foundation.

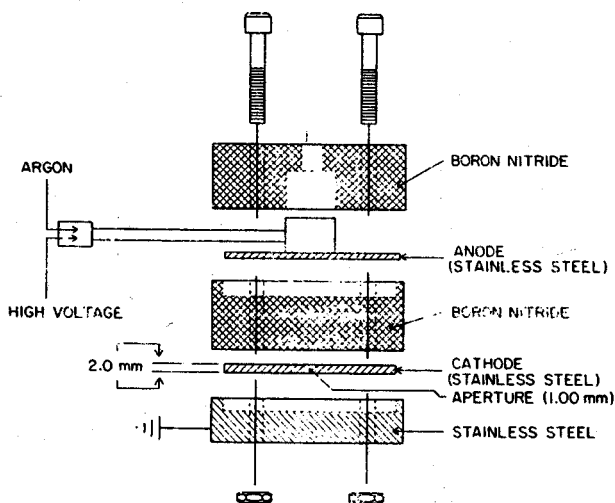


Fig. 1. Schematic assembly drawing indicating the components of the glow discharge ion source.

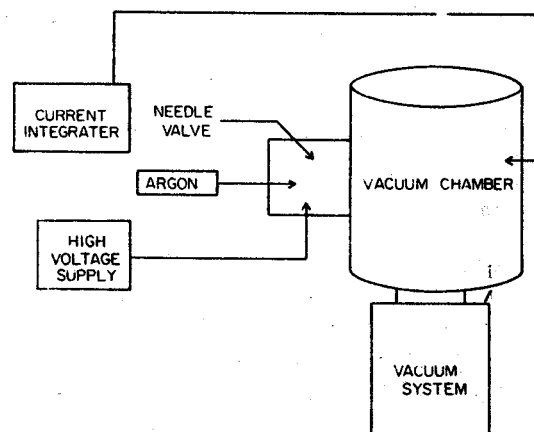


Fig. 2. Block diagram of the external components of the ion beam sputtering system.

A constraint on the universal baryon density from the abundance of ${}^7\text{Li}$

THE observed interstellar abundance of ${}^2\text{H}$ has been used^{1,2} to estimate the mean baryon density (ρ_b) of the Universe. This follows, because (1) there is no plausible source for ${}^2\text{H}$ other than the primordial big bang and (2) the production of ${}^2\text{H}$ in a standard big bang decreases rapidly with increasing ρ_b . If one then assumes that all ${}^2\text{H}$ was formed in a big bang, the observed abundance² of this nuclide requires a value of ρ_b sufficiently low¹ that, for a cosmological constant $\Lambda=0$, the present expansion of the Universe will continue forever and the Universe is open. A major weakness in this argument is that another source of ${}^2\text{H}$ may be found. It has been suggested, for example, that ${}^2\text{H}$ could be made in shock waves accompanying a supernova explosion; this now seems unlikely³, but other mechanisms will certainly be suggested, so that it is important to obtain confirmation of the above conclusion. The predicted production of ${}^7\text{Li}$ in a big bang² varies rapidly with ρ_b and could be used to estimate ρ_b if the fraction of the observed ${}^7\text{Li}$ made in the big bang were known. Unfortunately there are many possible sources⁴ of ${}^7\text{Li}$ and such estimates must be regarded with scepticism. In this note we point out that ${}^7\text{Li}$ can be used to place an upper limit on ρ_b , even if other production mechanisms are important, and that this limit also strongly favours an open universe. This possibility arises because the big bang production of ${}^7\text{Li}$ increases with increasing ρ_b (for $\rho_b > 10^{-31}$) so that an upper limit is obtained by attributing all of the observed ${}^7\text{Li}$ to the big bang.

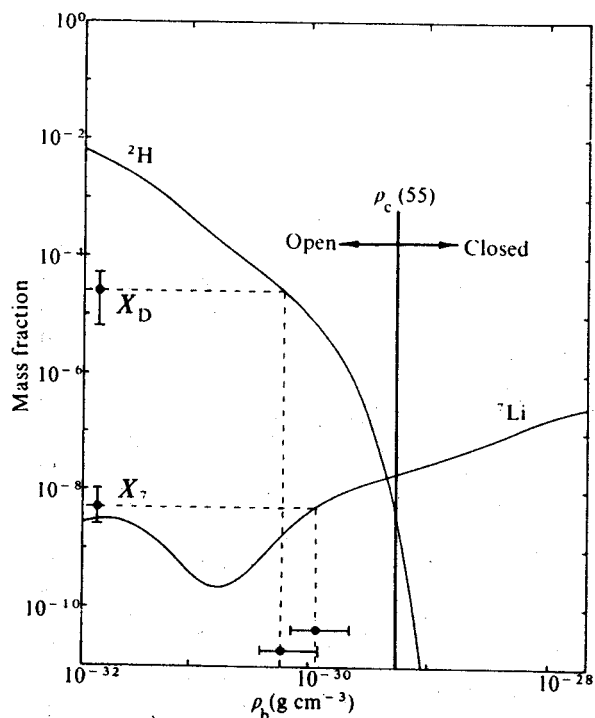


Fig. 1 Abundances of ${}^2\text{H}$ and ${}^7\text{Li}$ produced in a standard big bang (adapted from ref. 8. The present black body temperature is taken to be 2.90 K, see ref. 9.) The vertical line labelled ρ_c (55) is the density necessary to close a Friedman universe with $\Lambda=0$, if $H_0=55 \text{ km s}^{-1} \text{ Mpc}^{-1}$ (in general $\rho_c = 5.7 \times 10^{-30} (H_0/55)^2$). The point labelled X_7 is the mass fraction of ${}^7\text{Li}$ corresponding to the abundance given by Boesgaard⁵, while that labelled X_D is the mass fraction of ${}^2\text{H}$ from the summary of ref. 2. (This latter value is smaller than that used by Gott *et al.*¹, mostly because they include an estimate of the effects of astration). The uncertainty indicated for X_7 is a factor of two in either direction while that for X_D covers the range from a factor of four smaller to a factor of two larger¹⁰. Corresponding values of ρ_b and their uncertainties are also shown. The value of ρ_b determined from the ${}^7\text{Li}$ abundance is only an upper limit if there are significant sources of ${}^7\text{Li}$ other than the big bang.

We have adopted here Boesgaard's⁵ value of the Li abundance which yields⁶ a fractional abundance by mass of ${}^7\text{Li}$, $X_7 = 5 \times 10^{-9}$. Assuming the big bang must not synthesise more than this amount leads to $\rho_b \leq 1.1 \times 10^{-30} \text{ g cm}^{-3}$. As is shown in Fig. 1, this is substantially less than the critical value ρ_c necessary to close a $\Lambda=0$ Friedman universe.

The uncertainty in X_7 is perhaps a factor of two: the meteoritic value⁶, for example, is $X_7 = 8 \times 10^{-9}$. Substantially larger values have been seen⁵ in a small number of red giant stars, but these values presumably reflect a local production mechanism. Allowing for a factor of two uncertainty gives an upper limit closer to ρ_c , but still favouring an open and forever expanding universe.

The existence of mechanisms which destroy ${}^7\text{Li}$ weakens the limit on ρ_b since the big bang may then have made more ${}^7\text{Li}$ than is now observed; conversely, discovery of additional sources of ${}^7\text{Li}$ strengthens the limit. Astration of primordial material is presumably the most important destruction process. Estimates of the fraction of matter which has passed through stars are rather uncertain but are typically about 0.5. It has been pointed out^{4,7}, however, that infall of primordial material from the galactic halo may be significant and would tend to compensate for the effects of astration for those nuclei produced in the big bang. Other sources of ${}^7\text{Li}$ are generally rather speculative⁴, except for production in the cosmic rays which yields roughly 10% of the observed ${}^7\text{Li}$. Since these various effects tend to offset each other, the observed value of X_7 seems reasonable but subject to uncertainty.

If it is a good approximation to ignore both astration and sources of ${}^2\text{H}$ and ${}^7\text{Li}$ other than the big bang, their observed abundances each separately determine the density. An estimate based on the ${}^2\text{H}$ abundance X_D is shown in Fig. 1, and is in good agreement with the density obtained from ${}^7\text{Li}$. Effects of astration would tend to worsen this agreement. Thus when other possible contributions to ${}^7\text{Li}$ are better understood, the requirement that the big-bang contribution to X_7 and X_D yield the same value of ρ_b may be a strong constraint on allowable astration.

We assumed above that the cosmological constant $\Lambda=0$. While this is consistent with the available data, a non-zero value cannot be excluded, except on aesthetic grounds, and its effects must be considered. It has been found¹¹ that for reasonable values of Λ , the limits on ρ_b from the ${}^2\text{H}$ and ${}^7\text{Li}$ abundances are essentially unchanged. But, the simplest relationship between ρ_b and the curvature and evolution of the Universe is no longer valid¹¹.

In summary, the simplest and most straightforward assumptions concerning the origin of ${}^7\text{Li}$ and the nature of the big bang expansion require an upper limit for the present universal density of $\rho_b = (1.1 [+1.1 \text{ or } -0.4]) \times 10^{-30} \text{ g cm}^{-3}$. Given that the Universe is indeed a Friedman universe with zero cosmological constant, the agreement between the present limit and that based on ${}^2\text{H}$ strongly supports the conclusion of Gott *et al.*¹ that the Universe is open and will continue to expand forever.

This research was supported by the USNSF.

Note added in proof: It has come to our attention that conclusions similar to those reached here have been discussed by G. Steigman at the Harvard Neighborhood Meeting on Cosmology, October 1975.

SAM M. AUSTIN
C. H. KING

Cyclotron Laboratory and Physics Department,
Michigan State University,
East Lansing, Michigan 48824

Received 27 June; accepted 15 August 1977.

- Gott, J. R., Gunn, J. E., Schramm, D. N. & Tinsley, B. M. *Astrophys. J.* **194**, 543-553 (1974).
- Schramm, D. N. & Wagoner, R. V. *A. Rev. nucl. Sci.* (in the press).
- Epstein, R., Arnett, W. D. & Schramm, D. N. *Astrophys. J. Suppl.* **31**, 111-141 (1976).
- Reeves, H. *A. Rev. Astr. Astrophys.* **12**, 437-469 (1974).
- Boesgaard, A. M. *Pub. astr. Soc. Pac.* **88**, 353-66 (1976).
- Cameron, A. G. W. *Space Sci. Rev.* **15**, 121-46 (1973).
- Audouze, J. & Tinsley, B. M. *Astrophys. J.* **192**, 487-500 (1974).
- Wagoner, R. V. *Astrophys. J.* **179**, 343-360 (1973).
- Woody, D. P., Mather, J. C., Nishioka, N. S. & Richards, P. L. *Phys. Rev. Lett.* **34**, 1036-1039 (1975).
- York, D. G. & Rogerson, J. B. Jr. *Astrophys. J.* **203**, 378-385 (1976).
- Tinsley, B. M. *Phys. Today* **30**, 32-38 (1977).

Fluctuations in Inelastic Proton Scattering from ^{58}Ni in the Energy Range 17.1 to 20.6 MeV

A.D. Frawley*, G.M. Crawley** and C.L. Hollas***

Department of Nuclear Physics, The Australian National University,
Canberra, Australia

Received November 22, 1977

Excitation functions of proton elastic and inelastic scattering on ^{58}Ni have been measured for proton energies in the range 17.1 to 20.6 MeV, at laboratory angles of 90° , 120° and 155° . All show cross section fluctuations. Excitation functions are presented for the elastic and for five inelastic groups in the energy range 18.1 to 18.59 MeV. These were analyzed by the Fourier analysis method, and the average level width found to be about 13 keV. The observation of strong fluctuations in the higher inelastic yields has implications for several microscopic analyses reported in the literature of $^{58}\text{Ni}(p, p')$ data obtained at 17.7 MeV incident proton energy.

Nuclear Reactions. $^{58}\text{Ni}(p, p)$, (p, p') , $E_p = 17.1 - 20.6$ MeV, ^{59}Cu deduced Γ .
Enriched target.

1. Introduction

Recently, there has been a number of microscopic analyses [1–5] of inelastic proton scattering [5, 6, 7] to unnatural parity final states. Interest in these transitions comes from the expectation [1, 5] that some unnatural parity states might be described by quite simple shell model wave functions. Therefore, one may hope to obtain unambiguous information about the details of the reaction mechanism, even in medium to heavy nuclei where few excited states are describable in terms of simple shell model wave functions. Also, to first order, these transitions do not involve the normally dominant spin-independent central part of the effective interaction, and so they allow a more sensitive investigation of the other contributions to the effective interaction. A microscopic analysis [2] of the inelastic scattering [6] of 17.7 MeV protons to the 1^+ state at 2.902 MeV and the 3^+ states at 3.420 and 3.775 MeV in ^{58}Ni has been reported. Exchange effects were treated in an approximate way in this analysis. The predicted cross sec-

tions were several orders of magnitude too small, and the shapes of the angular distributions could not be reproduced over the entire angular range. The same data for the 3^+ state at 3.414 MeV were used in a later study [3] of the effect of velocity dependence in the two-body force. The angular distribution was not reproduced by any of the calculations. In contrast to these results, a microscopic analysis [5] of the inelastic scattering of 17.2 MeV protons to the 1^+ state at 3.487 MeV and to the 3^+ state at 3.635 MeV in ^{88}Sr gave a good account of the data. In a recent re-analysis [1] of the data from 17.7 MeV inelastic scattering to the 1^+ state at 2.90 MeV in ^{58}Ni , the discrepancies mentioned above were removed by including exchange core polarization contributions, in the form of two-step resonance processes [4] in a microscopic antisymmetrized distorted wave calculation. Most of the cross section strength in this calculation came from the two-step resonance process, the valence-direct and valence-exchange contributions being much too small to account for the measured cross section. No allowance was made in any of the above analyses for statistical compound nuclear contributions.

The initial aim of the present work was to provide

* Present address: Florida State University, Tallahassee, FL

** On sabbatical leave from Michigan State University. Research supported in part by U.S. National Science Foundation

*** Present address: Los Alamos Scientific Laboratory, Los Alamos, NM, USA

Unified Model of Deep Inelastic Heavy Ion Collisions: Collectivity and Statistics*

C.M. Ko

Physics Department, Michigan State University, East Lansing, Michigan, USA

Received January 29, 1978

Deep inelastic heavy ion collisions are viewed as multi-step processes described in terms of coupled-channel equations. Including both statistical and collective excitations, it is shown that in the semi-classical limit the coupled-channel equations reduce to a classical equation of motion for the relative coordinate with frictional force, master equation for the intrinsic occupation probabilities, and a damped forced harmonic oscillation for the mean deformation of the ions. We therefore succeed in unifying the approaches of Agassi et al. and Broglia et al., and in justifying the phenomenological models of Deubler et al. and Abul-Magd et al.

The study of deep inelastic heavy ion collisions in the framework of coupled-channel equations follows two different approaches. Agassi et al. [1] assumes that the intrinsic excitations are statistical and describable in terms of a random-matrix model. In the semi-classical limit, they obtain the classical friction model of Gross et al. [2] with the frictional coefficient determined by the statistical input. On the other hand, Broglia et al. [3] treat the intrinsic excitations as collective vibrations described as damped forced harmonic oscillations with the mass parameter, the restoring force and the damping coefficient taken from experimental information. In the model of Agassi et al. the relative kinetic energy is transferred directly to the complicated intrinsic excitations, while in the model of Broglia et al. it is first transferred to collective excitations which are then dissipated into the complicated intrinsic states. In the phenomenological models of Deubler and Dietrich [4] and Abul-Magd et al. [5], they have demonstrated via classical frictional model that both friction and deformation (or equivalently collective excitations) play important roles in the damping of the relative motion. It is therefore most desirable to unify the approaches of Agassi et al. and Broglia et al., and to justify the phenomenological models of Deubler et al. and Abul-Magd et al.

There are microscopic methods of treating the coupling between collective (other than the relative coordinate) and intrinsic degrees of freedom. Hofmann and Siemens [6] use the linear response theory and Ayik and Nörenberg [7] use the method of non-equilibrium quantum statistics. In both cases, the collective degree of freedom is treated like a relative coordinate. These approaches are very different from ours in that we consider the collective degrees of freedom at the same footing as the intrinsic degrees of freedom.

We shall follow the method of Ko et al. [8]. For simplicity, we restrict ourselves to the one-dimensional geometry for the relative motion and neglect the transfer of nucleons as in [8]. Also, we allow only the target to be excited to simplify the notation. The Hamiltonian which describes the two colliding nuclei is written in the following form

$$H(x, \alpha, \xi) = T(x) + h_1(\alpha) + h_2(\xi) + V_1(x, \xi) + V_2(x, \alpha) + V_3(\alpha, \xi) \quad (1)$$

where $T(x)$ is the kinetic energy operator for the relative motion, $h_1(\alpha)$ and $h_2(\xi)$ the collective and intrinsic Hamiltonians respectively, $V_3(\alpha, \xi)$ the coupling between the collective and the intrinsic degrees of freedom, $V_1(x, \xi)$ and $V_2(x, \alpha)$ the relative–intrinsic and relative–collective couplings respectively. Let the collective and intrinsic spectra be

* Work supported by the National Science Foundation

The Pathways of Assimilation of $^{13}\text{NH}_4^+$ by the Cyanobacterium, *Anabaena cylindrica**

(Received for publication, May 2, 1977)

JOHN C. MEEKS,† C. PETER WOLK,§ JOSEPH THOMAS,¶ WOLFGANG LOCKAU,|| AND PAUL W. SHAFFER
From the MSU/ERDA Plant Research Laboratory, Michigan State University, East Lansing,
Michigan 48824

SAM M. AUSTIN, WAN-SHEN CHIEN, AND AARON GALONSKY
From the Cyclotron Laboratory and Department of Physics, Michigan State University, East Lansing,
Michigan 48824

The principal initial product of metabolism of ^{13}N -labeled ammonium by *Anabaena cylindrica* grown with either NH_4^+ or N_2 as nitrogen source is amide-labeled glutamine. The specific activity of glutamine synthetase is approximately half as great in NH_4^+ -grown as in N_2 -grown filaments. After 1.5 min of exposure to $^{13}\text{NH}_4^+$, the ratio of ^{13}N in glutamate to ^{13}N in glutamine reaches a value of approximately 0.1 for N_2 - and 0.15 for NH_4^+ -grown filaments, whereas after the same period of exposure to $[^{13}\text{N}]\text{N}_2$, that ratio has reached a value close to unity and is rising rapidly. During pulse-chase experiments, ^{13}N is transferred from the amide group of glutamine into glutamate, and then apparently into the α -amino group of glutamine. Methionine sulfoximine, an inhibitor of glutamine synthetase, inhibits the formation of glutamine. In the presence of the inhibitor, direct formation of glutamate takes place, but accounts for only a few per cent of the normal rate of formation of that amino acid; and alanine is formed about as rapidly as glutamate. Azaserine reduces formation of $[^{13}\text{N}]\text{glutamate}$ approximately 100-fold, with relatively little effect on the formation of $[^{13}\text{N}]\text{glutamine}$. Aminooxyacetate, an inhibitor of transaminase reactions, blocks transfer of ^{13}N to aspartate, citrulline, and arginine. We conclude, on the basis of these results and others in the literature, that the glutamine synthetase/glutamate synthase pathway mediates most of the initial metabolism of ammonium in *A. cylindrica*, and that glutamic acid dehydrogenase and alanine dehydrogenase have only a very minor role.

In *Anabaena cylindrica*, the major enzymatic pathway for the assimilation of NH_4^+ derived from N_2 consists of glutamine synthetase and glutamate synthase (1, 2). This pathway was previously shown to be the major route of assimilation of N_2 -derived ammonium in heterotrophic nitrogen-fixing bacteria (3, 4) and of exogenous ammonium by nitrogen-limited chemostat cultures of marine pseudomonads (5) and *Rhizobium* (6). The levels of extractable activities of glutamine synthetase and glutamate synthase decline during growth with high levels of exogenous ammonium, while the level of extractable glutamic acid dehydrogenase activity increases (5, 6; cf. Ref. 4). The alteration in the activities of extractable enzymes has been taken to indicate that the major route of ammonium assimilation changes from the glutamine synthetase/glutamate synthase pathway to catalysis by glutamic acid dehydrogenase (7). In contrast to the results just cited, enzymological studies of *A. cylindrica* have indicated that the extractable activity of glutamine synthetase remains high in ammonium-grown (8, 9) and N_2 -grown, ammonium-treated (10) cultures, compared to untreated, N_2 -grown cells. These data imply that glutamine continues to be synthesized by glutamine synthetase in NH_4^+ -grown as well as N_2 -grown cells of *A. cylindrica*.

The specific activities of glutamic acid dehydrogenase (NADPH) which have been reported in *A. cylindrica* (11) and *Anabaena variabilis* (12) are rather low; the level of this enzyme is greater in nitrate-grown than in N_2 -grown *Gloeocapsa* strain 6909 (13). Alanine dehydrogenase is relatively active in *A. cylindrica*, although with a low affinity for ammonium, and the specific activity increases in N_2 -fixing and nitrogen-starved cultures compared to NH_4^+ -grown cells (14). It is not known whether in the cyanobacteria these dehydrogenases function in an assimilatory or dissimilatory manner. It is also unknown whether glutamate synthase activity (15) is present in ammonium-grown cyanobacteria.

Much, perhaps all, of dinitrogen assimilation by *A. cylindrica* takes place in differentiated cells called heterocysts (16-18), where it is coupled to synthesis of glutamine (18). Glutamine synthetase of N_2 -grown filaments is present largely in the vegetative cells, although it is also present in heterocysts and in fact at higher specific activity (10, 18); glutamate synthase appears to be present essentially only in vegetative cells (18). Ammonium is maintained at a very low intracellular concentration during N_2 fixation (1). However,

* This research was supported by the United States Energy Research and Development Administration under Contract EY-76-C-02-1338, and by the United States National Science Foundation. The costs of publication of this article were defrayed in part by the payment of page charges. This article must therefore be hereby marked "advertisement" in accordance with 18 U.S.C. Section 1734 solely to indicate this fact.

† Permanent address, Department of Bacteriology, University of California, Davis, Calif. 95616.

§ To whom inquiries concerning this paper should be addressed.

¶ Permanent address, Biology and Agriculture Division, Bhabha Atomic Research Centre, Trombay, Bombay 400 085, India.

|| Permanent address, Fachbereich Biologie und Vorklinische Medizin, Institut für Botanik, Universität Regensburg, Universitätsstr. 31, D8400 Regensburg, Federal Republic of Germany.

Pathways of Assimilation of [^{13}N]N $_2$ and $^{13}\text{NH}_4^+$ by Cyanobacteria with and without Heterocysts

JOHN C. MEEKS,† C. PETER WOLK,^{1*} WOLFGANG LOCKAU,†† NORBERT SCHILLING,¹ PAUL W. SHAFFER,¹ AND WAN-SHEN CHIEN²

MSU-ERDA Plant Research Laboratory¹ and Cyclotron Laboratory and Department of Physics,² Michigan State University, East Lansing, Michigan 48824

Received for publication 9 January 1978

The principal initial product of metabolism of [^{13}N]N $_2$ and $^{13}\text{NH}_4^+$ by five diverse cyanobacteria is glutamine. Methionine sulfoximine inhibits formation of [^{13}N]glutamine except in the case of *Gloeotheca* sp., an organism with a thick sheath through which the inhibitor may not penetrate. Thus, glutamine synthetase appears to catalyze the initial step in the assimilation of N $_2$ -derived or exogenous NH $_4^+$ by these organisms. [^{13}N]Glutamate is, in all cases, the second major product of assimilation of ^{13}N -labeled N $_2$ and NH $_4^+$. In all of the N $_2$ -fixing cyanobacteria studied, the fraction of ^{13}N in glutamine declines and that in glutamate increases with increasing times of assimilation of [^{13}N]N $_2$ and $^{13}\text{NH}_4^+$, and (*Gloeotheca* again excepted) methionine sulfoximine reduces incorporation of ^{13}N into glutamate as well as into glutamine. Glutamate synthase therefore appears to catalyze the formation of glutamate in a wide range of N $_2$ -fixing cyanobacteria. However, the major fraction of [^{13}N]glutamate formed by *Anacystis nidulans* incubated with $^{13}\text{NH}_4^+$ may be formed by glutamic acid dehydrogenase. The formation of [^{13}N]alanine from $^{13}\text{NH}_4^+$ appears to be catalyzed principally either by alanine dehydrogenase (as in *Cylindrospermum licheniforme*) or by a transaminase (as in *Anabaena variabilis*).

Experiments using the radioisotope ^{13}N have shown that in the heterocyst-forming cyanobacterium *Anabaena cylindrica* the major enzymatic pathway for the assimilation of NH $_4^+$, whether derived from N $_2$ or supplied exogenously, consists of glutamine synthetase (L-glutamate:ammonia ligase [ADP forming], EC 6.3.1.2) and glutamate synthase (L-glutamate:ferredoxin oxidoreductase [transaminating], EC 1.4.7.1) (11, 19). Glutamic acid dehydrogenase and alanine dehydrogenase also function in the assimilation of exogenously supplied NH $_4^+$ in this cyanobacterium, but at a much lower rate even in the presence of relatively high levels of NH $_4^+$ (11). In this respect, *A. cylindrica* differs from some heterotrophic, dinitrogen-fixing bacteria in which N $_2$ -derived NH $_4^+$ is assimilated principally by the glutamine synthetase/glutamate synthase pathway, whereas, during growth in the presence of high exogenous concentrations of NH $_4^+$, the NH $_4^+$ is assimilated via glutamic acid dehydrogenase (6).

When *A. cylindrica* is grown aerobically,

much, and perhaps all, of the dinitrogen reduction occurs in the heterocysts, where it is coupled to the formation of glutamine by the action of glutamine synthetase (17). Glutamate synthase-mediated formation of glutamate appears to occur only in vegetative cells of N $_2$ -grown filaments, whereas glutamine synthetase functions in both cell types (17).

The pattern of positioning of heterocysts in cyanobacteria varies among different genera. For example, spaced sequences of intercalary heterocysts are present in *Anabaena*, whereas only terminal heterocysts are normally found in *Cylindrospermum*. In addition, nitrogenase activity in the cyanobacteria is not confined to heterocyst-forming species. Thus, *Plectonema boryanum* reduces acetylene and grows with N $_2$ as the sole nitrogen source under microaerobic conditions (16), and *Gloeocapsa* sp. can reduce acetylene and grow with N $_2$ as the sole nitrogen source aerobically (20; and cf. 7). Yet other cyanobacteria, e.g., *Anacystis nidulans* (syn. *Synechococcus* 6301 [15]), appear unable to reduce acetylene or N $_2$. *Anabaena*, *Cylindrospermum*, and *Plectonema* are filamentous, *Gloeocapsa* is colonial or unicellular, and *Anacystis* is unicellular. We have sought to determine whether the diversity of morphological and physiological

† Present address: Department of Bacteriology, University of California, Davis, CA 95616.

†† Present address: Fachbereich Biologie und Vorklinische Medizin, Institut für Botanik, Universität Regensburg, D-8400 Regensburg, Federal Republic of Germany.

Initial Organic Products of Fixation of [^{13}N]Dinitrogen by Root Nodules of Soybean (*Glycine max*)¹

Received for publication January 9, 1978 and in revised form February 20, 1978

JOHN C. MEEKS,² C. PETER WOLK,³ NORBERT SCHILLING, AND PAUL W. SHAFFER
MSU-ERDA Plant Research Laboratory

Yael AVISSAR
Department of Botany and Plant Pathology

WAN-SHEN CHIEN
Cyclotron Laboratory, Michigan State University, East Lansing, Michigan 48824

ABSTRACT

When detached soybean *Glycine max* (L.) Merr. cv. Hark, nodules assimilate [^{13}N]N₂, the initial organic product of fixation is glutamine; glutamate becomes more highly radioactive than glutamine within 1 minute; ^{13}N in alanine becomes detectable at 1 minute of fixation and increases rapidly between 1 and 2 minutes. After 15 minutes of fixation, the major ^{13}N -labeled organic products in both detached and attached nodules are glutamate and alanine, plus, in the case of attached nodules, an unidentified substance, whereas [^{13}N]glutamine comprises only a small fraction of organic ^{13}N , and very little ^{13}N is detected in asparagine. The fixation of [^{13}N]N₂ into organic products was inhibited more than 99% by C₂H₂ (10%, v/v). The results support the idea that the glutamine synthetase-glutamate synthase pathway is the primary route for assimilation of fixed nitrogen in soybean nodules.

Ammonium is the initial product of dinitrogen fixation by symbiotic (1) and free-living (19, 21) prokaryotes and by nitrogenase *in vitro* (16). Activities of the ammonium-assimilating enzymes glutamic acid dehydrogenase and glutamine synthetase, as well as glutamate synthase, have been detected in bacteroid fractions isolated from root nodules of soybean (2, 3) and lupin (2, 9). Nevertheless, free-living N₂-fixing *Rhizobium japonicum* and bacteroids of *R. japonicum* isolated from soybean release 90 to 94% of the products of fixation of $^{15}\text{N}_2$ into the medium as ammonium (1, 13). Dilworth and Brown (2) suggested that ammonium produced by bacteroids is assimilated in nodules through either the glutamine synthetase-glutamate synthase or glutamic acid dehydrogenase pathways, and favored the latter. In serradella, the major amino acids formed from $^{15}\text{N}_2$ were glutamate and glutamine, but the initial organic product, and thereby the primary assimilatory route, was not determined (8). The form in which nitrogen is translocated from the nodules to the root and shoot of the host plant has not been directly identified, but is assumed to

be asparagine, based on analysis of compounds in the bleeding sap (4, 14, 17, 23).

In this study we identify glutamine as the initial organic product of fixation of [^{13}N]N₂ ($t_{1/2}$ [^{13}N] = 10 min) by detached soybean nodules. However, the major organic products that accumulate after 15 min of fixation of [^{13}N]N₂ are glutamic acid and alanine, with minimal amounts of glutamine. After 6 or 15 min of fixation of [^{13}N]N₂ by nodules attached to seedlings, these two amino acids and, in addition, an unidentified substance are highly labeled.

MATERIALS AND METHODS

Plant and Bacterial Strains, and Growth Conditions. Yeast extract-mannitol medium (YM) contains, in g/l: mannitol, 10; yeast extract (Difco), 1; K₂HPO₄, 0.5; MgSO₄·7H₂O, 0.2; NaCl, 0.1; and CaSO₄·2H₂O, 0.1. *Rhizobium japonicum* strain 311b-110, kindly supplied by K. D. Nadler, Department of Botany and Plant Pathology, Michigan State University, was maintained on YM agar (1.5%) slants and transferred every 3 months. Liquid cultures, started from slants in 20 ml of YM medium, were transferred to 500 ml of YM medium in 1-liter flasks, and were aerated by agitation on a reciprocating shaker. Cells from 2-day-old cultures were harvested by centrifugation at 6,000g for 10 min, washed and resuspended in ("N-free") legume nutrient medium free of combined nitrogen (6), and used as inoculum.

Glycine max (L.) Merr. cv. Hark seeds were surface-disinfected for 20 sec with 1% NaOCl, washed in running tap water, and planted in a Vermiculite-Perlite bed. The bed was inoculated with the *Rhizobium* suspension. Aerated N-free medium was circulated through the bed of germinating seeds for 1 week. The beds were illuminated with two 40-w Gro-lux fluorescent lamps (Westinghouse Electric Corp., Bloomfield, N.J.) at a distance of 60 cm. Inoculated seedlings were transferred to pots (five/pot) containing a mixture of Vermiculite and Perlite and grown in a greenhouse with supplementary illumination from four 40-w Gro-lux fluorescent lamps at a distance of 35 to 45 cm. Seedlings were watered with N-free medium. Under these inoculation conditions, nodules form predominantly at the crown of the root (12). Seedlings 2.5 to 5 weeks old, and nodules from such seedlings, were used in these experiments.

Acetylene Reduction. Detached nodules were placed in 5-ml vials which were then sealed with a serum stopper. The vials were evacuated three times and filled to atmospheric pressure with Ar/O₂/CO₂ (80:19:1, v/v/v). Acetylene was injected to a final concentration of 0.006% (v/v) (60 $\mu\text{l/l}$), or 6% (v/v) (60 ml/l). When 6% C₂H₂ was used, 40 μl of the atmosphere was analyzed for C₂H₄ with a Varian Aerograph model 1200 gas chromatograph.

¹ This research was supported by the United States Energy Research and Development Administration under Contract EY-76-C-02-1338, and by the National Science Foundation. Y. A. was supported by National Science Foundation Grant PCM-76-22793 to K. D. Nadler. N. S. received partial support from the Deutsche Forschungsgemeinschaft.

² Present address: Department of Bacteriology, University of California, Davis, California 95616.

³ To whom requests for reprints should be sent.

RADIOCHEMISTRY AND RADIOPHARMACEUTICALS

Tantalum-178—A Short-Lived Nuclide for Nuclear Medicine: Production of the Parent W-178

B. Leonard Holman, Gale I. Harris, Rudi D. Neirinckx, Alun G. Jones, and John Idoine

*Harvard Medical School and Peter Bent Brigham Hospital, Boston, Massachusetts
and Michigan State University, East Lansing, Michigan*

The physical decay characteristics of the short-lived radionuclide Ta-178 (half-life 9.3 min) appear to be suitable for use in conjunction with low-energy detection systems such as the multiwire proportional camera. This camera is inefficient for emissions with energies greater than 100 keV. The gamma-ray spectrum of Ta-178 is dominated by the characteristic hafnium x-rays (55–65 keV), emitted as a result of electron-capture decay. The parent nuclide, W-178 (half-life 21.7 d), was produced in the Michigan State University cyclotron by proton bombardment of stacked natural tantalum-foil targets. Optimum production was found to occur with an incident proton energy of 34 MeV at an effective activity of 1.1 mCi/ μ A-hr per MeV of target thickness. Tungsten-178 was chemically separated from the Ta foils with a yield of 98%.

J Nucl Med 19: 510–513, 1978

The high-pressure multiwire proportional camera (MWPC) has recently attracted attention as a possible alternative to the gamma camera because it provides high spatial resolution at count rates more than twice those of present detectors (1). This system is designed for use with low-energy gamma emitters: for example, the efficiency is typically 25% at 140 keV, 70% at 80 keV and 80% at 60 keV (2). This paper reports on a short-lived radionuclide, tantalum-178 (Ta-178), which may be suitable for use with such a camera.

Tungsten-178 ($T_{1/2} = 21.7$ d) decays entirely by electron capture to the 9.3-min Ta-178 daughter (Fig. 1) without feeding the high-spin Ta-178 isomer ($T_{1/2} = 2.2$ hr). The short-lived Ta-178 then decays to stable hafnium-178, 99.2% of the time by electron capture and 0.81% by positron emission. Electron capture results in a 61.2% branch to the ground state of Hf-178 and 33.7% to the first excited state at 93.1 keV; a 93.1 keV photon is emitted in 5.9% of the disintegrations (Fig. 2). The remaining 4.3% feeds hafnium levels between 1175 and 1772 keV. Since the 93-keV transition is heavily converted,

the most prominent features of the Ta-178 emission spectrum are the characteristic radiation peaks of hafnium, with energies between 54.6 and 65.0 keV (3,4).

This communication deals with the production of the parent radionuclide, W-178.

MATERIALS AND METHODS

The reaction chosen was $^{181}\text{Ta}(p,4n)^{178}\text{W}$. This is the one used by Siddiqi and Emery (5) to produce samples for spectroscopic studies, but little information was available concerning production rates. Preliminary calculations based on the nuclear evaporation code ALICE (6) predicted an energy-dependent cross-section, approximately Gaussian in shape, centered at an incident proton energy $E_p = 34$ MeV. For comparison, the results of Rao et al. (7) and Birattari et al. (8) indicated that optimum produc-

Received Nov. 7, 1977; revision accepted Dec. 23, 1977.

For reprints contact: B. Leonard Holman, Dept. of Radiology, Harvard Medical School, 25 Shattuck St., Boston, MA 02115.